RETROSPECTIVE ANALYSIS OF TWO NORTHERN CALIFORNIA WILD-LAND FIRES VIA LANDSAT FIVE SATELLITE IMAGERY AND NORMALIZED DIFFERENCE VEGETATION INDEX (NDVI)

A Thesis

Presented

to the Faculty of

California State University, Chico

In Partial Fulfillment

of the Requirements for the Degree

Master of Science

in

Biological Sciences

---

by

Bennett R. Sall

Fall 2012

RETROSPECTIVE ANALYSIS OF TWO NORTHERN CALIFORNIA WILD-LAND FIRES VIA LANDSAT FIVE SATELLITE IMAGERY AND NORMALIZED DIFFERENCE VEGETATION INDEX (NDVI)

A Thesis

by

Bennett R. Sall

Fall 2012

APPROVED BY THE DEAN OF GRADUATE STUDIES
AND VICE PROVOST FOR RESEARCH:

_____
Eun K. Park, Ph.D.

APPROVED BY THE GRADUATE ADVISORY COMMITTEE:

_____
James C. Pushnik, Ph.D., Chair

_____
Patricia Edelmann, Ph.D.

_____
David L. Brown, Ph.D.

TABLE OF CONTENTS

LIST OF TABLES

TABLE PAGE

LIST OF FIGURES

ABSTRACT

RETROSPECTIVE ANALYSIS OF TWO NORTHERN CALIFORNIA WILD-LAND FIRES VIA LANDSAT FIVE SATELLITE IMAGERY AND NORMALIZED DIFFERENCE VEGETATION INDEX (NDVI)

by

Bennett R. Sall

Master of Science in Biological Sciences

California State University, Chico

Fall 2012

Wild-land fires are a dynamic and destructive force in natural ecosystems. In recent decades, fire disturbances have increased concerns and awareness over significant economic loss and landscape change. The focus of this research allowed for the utilization of Landsat 5 imagery, analysis software, and ground based methods to study two northern California wild-land fires: Butte Humboldt Complex (BHC) and Butte Lightning Complex (BLC) of 2008. Multi-temporal and NDVI satellite imagery were used to visually assess levels of landscape change, under two temporal scales. Visual interpretation indicated noticeable levels of landscape change and relevant insight into the magnitude and impact of both wild-land fires. Satellite NDVI, local temperature, and precipitation time-based (1998-2010) data were incorporated to

contrast pre- and post-wild-land fire vegetation response and recovery. NDVI trends may have been influenced by low precipitation, substrate flammability, and vegetation accumulation. Statistical analysis using Coefficient of Determination R^2 comparison of satellite to ground based NDVI, resulted in weak linear correlations for BHC (R^2 = 0.0859) and Richardson Springs (R^2 = 0.3555), in contrast to a slightly negative correlation for BLC (R^2 = 0.001).

Normalized Burn Ratio (NBR) and delta NBR data allowed for quantitative analysis of burn severity levels. Delta NBR results indicated unburned, low severity, and low re-growth for BHC “burned center” subplots. In contrast, delta NBR values for BLC “burned center” subplots indicated low and mid to high burn severity levels. Examination pre- and post-wild-land fire vegetation demonstrated potential for wild-land fires and associated influences to be detected by way of remote sensing technology.

CHAPTER I

INTRODUCTION

Wild-land Fire Prevalence and Historical Evolution

Fire regimes have changed across the country as well as in northern California forests because of policies and management practices associated with fire suppression (Skinner and Chang 1996). Fire regimes can be defined as the characteristics and patterns of fires that occur in a specific area over time (Skinner and Chang 1996). Consideration of fire regimes has been an instrumental process for forest managers and fire ecologists to better understand and manage fire prone areas (Conedera *et al.* 2008). Fire suppression policies gained momentum as fire was perceived by the public as destruction of natural areas (Skinner and Chang 1996). Economics also played a part in that trees with fire damage were seen as less valuable and thus fires caused a reduction in the number of trees that could be logged (Skinner and Chang 1996). Before fire suppression policies were put in to place in the early nineteen hundreds, fire regimes in northern California forests were made up of mostly low to medium severity fires, but due to fire suppression, there has been a shift towards high severity fires (Skinner and Chang 1996). With fewer fires, there is a build-up of materials that would normally have been burned under pre-suppression policies (Skinner and Chang 1996). Currently, when fires do occur they have substantially more fuel and thus higher severity (Skinner and Chang 1996). Also, another

factor that influenced higher severity fires was the length of burn time (Skinner and Chang 1996). Before fire suppression, fires could burn for long periods of time, such as months, while after suppression was implemented fires were extinguished as quickly as possible, thus reducing the amount of fuel burned (Skinner and Chang 1996).

Fire suppression policies have changed over time and in the 1970s and 1980s, the US Forest Service became more informed about fires in relevance to ecosystem processes and functionality (Kneeshaw *et al.* 2004). Currently, where possible they let forest fires burn in a more natural way, without being quickly extinguished (Kneeshaw *et al.* 2004). Also, Forest Service officials adopted the idea that forest fires could be less severe with fuel load reduction using prescribed fires and thinning (Ritchie *et al.* 2007). In a study on effects of prescribed fires and thinning, forest areas that were first thinned to lower the risk of crown fires and then prescribed burns to remove ground fuel resulted in a significant reduction in fire severity, allowing a higher survival rate of trees compared to fire suppression practices (Ritchie *et al.* 2007).

Prescribed burns may also benefit the northern spotted owl (*Strix occidentalis*) (Kennedy *et al.* 2009). This is because the use of prescribed burns can reduce fire severity levels, providing increased protection to old-growth forest habitats (Kennedy *et al.* 2009). The use and benefit of prescribed fires can be somewhat limited because the northern spotted owl is on the federal threatened species list (Fry and Stephens 2006). For this reason, many forest areas of northern California, including Whiskeytown National Recreation Area Park in Klamath Mountains must get authorization for prescribed burns from the U.S. Fish and Wildlife Service on an individual basis (Fry and Stephens 2006). Also, other studies have shown that thinning and prescribed fires leave forest areas

different (Fry and Stephens 2006). Compared to natural fires, prescribed fires tend to be more uniform and less heterogeneous (Fry and Stephens 2006). Some researchers believe the best approach is to try and restore forest ecosystems by allowing fires to take their course, as observed before fire suppression was implemented (Fry and Stephens 2006).

Fire regimes have numerous dynamic aspects involved when trying to look at the overall picture (Conedera *et al.* 2008). Environmental factors such as climate and climate change have a great effect on fire regimes. There is a strong correlation between when fires will occur and the type of climate (Taylor and Beaty 2005). In the northern Sierra Nevada mountains, wild-land fires were more widespread and severe when oscillations in climate occurred (Taylor and Beaty 2005). For example, when wild-land fires were preceded by cooler years, allowing for wetter conditions causing increased vegetation growth, followed by warmer years where drought was a major factor, vegetation became drier, thereby increasing fuel for fires to burn (Taylor and Beaty 2005). Also, years that were preceded by warmer conditions associated with La Nina also showed a significant increase in the occurrence of wild-land fires (Taylor and Beaty 2005). Higher temperatures and lower humidity can contribute as well to increased fire severity (Taylor and Skinner 1998).

Some studies suggest that the effects of global warming on future fires in northern California will be significant (Fried *et al.* 2004). A study on impact of climate change on wildfire severity in northern California suggests that at double the CO2 rates, fires are estimated to spread faster and also roughly double the amount of non-contained or escaped fires than are seen presently (Fried *et al.* 2004). In addition to increased severity and fire frequency, there would also be a greater impact on grass and shrub areas

rather than low density forests (Fried *et al.* 2004). Another study involving the effects of climate change on fire regimes also illustrated that by 2050, there will be increased severity and frequency of fires (Whitlock *et al.* 2003). This study predicted that as temperature increased, it would cause drought-like conditions, which may influence moisture levels in plants as well as which type of plants will inhabit an area (Whitlock *et al.* 2003). The amount of vegetation moisture and type of vegetation present is directly correlated to the severity of a fire and how often an area will burn (Whitlock *et al.* 2003).

Native American Influences on Wild-land Fire

Native Americans have had a significant impact on fire regimes in California (Erlandson 1994). With widespread distribution throughout and larger populations located near the coastal, foothill, and valley areas (Erlandson 1994), they were effective in using fire to change the landscape for a variety of purposes (Keeley 2002). Many tribes in California lived near chaparral areas that were made up of species such as toyon (*Heteromeles arbutifolia*), scrub oak (*Quercus berberidifolia*), and Manzanita (*Arctostaphylos spp*.) with a vegetation pattern characterized spatially as dense with regions of impermeability (Keeley 2002). Native Americans preferred landscapes that had a mixture of both chaparral and grasslands because it gave them greater access to plant and animal resources (Keeley 2002). Animals such as black tailed deer (*Odocoileushemionus*) and rabbits (*Sylvilagus bachmani*) prefer this mixture of grassland and chaparral landscapes and were less abundant in less disturbed shrublands (Keeley 2002). Also, they relied on plant resources coming from the grasslands, such as chia seeds (*S. columbaria*) (Keeley and Fotheringham 1998). Travel through the dense

chaparral was difficult which in turn slowed the connectivity for the native people as well as medium to large animals (Keeley 2002).

For these reasons, Native Americans would set wild-land fires to properly thin the undisturbed chaparral and created more open space, allowing for better access to resources in the area (Keeley 2002). Post-wild-land fire recovery consisted of isolated fragmented shrub patches in areas dominated by grass and herbaceous ground cover (Keeley 2002). These landscape conversions to grasslands are best illustrated when repeated fires completely eliminate the shrubs and in a post wild-land fire environment, only annuals and herbs persist (Keeley 2000). Once an area had been burned, fire frequency decreased, however, to keep the grasslands from fully returning to the chaparral, a minimum fire frequency of every ten years was necessary (Keeley 2000).

With a mixture of chaparral and grasslands there was likely an increase in biodiversity as well as landscape heterogeneity (Keeley 2002). Chaparral areas were estimated to have twenty-four species per 0.1 hectare, while post-wild-land fire landscapes consists of over eighty species per 0.1 hectare, with a vast majority consisting of annuals (Keeley 2002). This resulted in a more diverse food supply, enabling sustainment of native populations in times of drought, which would have normally required them to migrate and find better habitats (Jones and Kennett 1999).

CHAPTER II

REMOTE SENSING AND REFLECTANCE

Technological advancements in recent decades in high resolution spectral imaging sensors and analysis software have permitted remote sensing to emerge as a valuable tool to comprehend, measure, and investigate a variety of different environments in a biological, physical, and chemical nature with high levels of accuracy and have been instrumental in gaining a better understanding of trends involved with vegetation physiology and plant stress (Rosso *et al.* 2005; Salazar *et al.* 2007; Horning *et al.* 2010; Ustin and Gamon 2010). In addition, it has been suggested that satellite remote sensing techniques are valuable in evaluating large ecosystems, such as the amount of land affected by the Humboldt and Butte County fire complexes of 2008, and may provide a better alternative to traditional field methods because it is less costly and destructive allowing for results to be obtained in a more timely manner for analysis (Inoue 2003; Rosso *et al.* 2005; Black and Guo 2008). In addition, remote sensing demonstrates unique abilities to detect vegetation stress and mortality, based on plant physiology and more specifically pigment deviations associated with chlorosis (Santos *et al.* 2010). This condition is induced by decreasing concentrations of chlorophyll a and b, in the red and blue visual spectrum regions (Santos *et al*. 2010). Such a decrease may be related to possible factors including but not limited to deficiencies concerning plant nutrients, herbivore interactions, and water stress (Santos *et al.* 2010).

Vegetation has been shown to display varying levels of reflectance and absorbance by rounded bell shaped reflection curves in the visual wavelength spectrum ranging from 0.400 to 0.800 μm (Lichtenhaler *et al.* 1998). This region's unique vegetation spectral signature may show variability in size and shape related to differences in chlorophyll concentrations (Lichtenhaler *et al.* 1998), and primarily decided by several pigments involved with photosynthesis (Ustin and Gamon 2010). For example, chlorophyll a and b have increased absorptions located in the blue (0.430 to 0.450 μm) and red (0.630 to 0.690 μm) ranges, with B-carotene peak absorption occurring at 0. 450 μm (Santos *et al.* 2010). Additionally, differences among *Pinus* spp. and more specifically the physical make of involved with leaf dimensions causing different rates of physiological decline, may have contributed to errors associated with reflectance comparisons in the visible wavelength regions (Santos *et al.* 2010). Also, at 0.700 μm, it was discovered that reflectance was increased in trees showing no visual symptoms in relation to non-living and stressed counterparts (Santos *et al.* 2010). Ground based methods, in contrast, have yielded similar results and have been effective in looking at several noteworthy vegetation reflectance trends (Zomer *et al.* 2009). For example, curves in the visible wavelength spectrum, associated with central green regions, have exhibited larger reflectance in relation to blue and red spectral regions, which typically show increased absorbance, due to photosynthetic activities and more specifically absorption by vegetation pigments (Zomer *et al.* 2009).

Plant physiology plays an important factor in reflectance measurements in the wavelengths ranging from 0.700 to 1500 μm, near infrared region, and can be related to dispersions within H_20 and air exchange regions and among leaves in canopy regions as

well as within the leaf structures (Ustin and Gamon 2010). These relationships enhance understanding perimeters at a canopy level, including area index of leaves, composition of plant materials, and distribution angles associated with leaf reflectance (Ustin and Gamon 2010). In contrast, in various regions across the spectrum, at leaf scale analysis, it is possible to detect a wide variety of characteristics including nitrogen, pigments such as anthocyanins, chlorophyll, carotenoids, plant materials such as lignocellulose, and water (Ustin and Gamon 2010). Also, signature spectral responses resulting from differences in growth patterns and individual variations in morphology of diverse vegetated landscapes, enabled remote sensing researchers to determine cover classifications (Ustin and Gamon 2010). More specifically, marshland and forest confer types exhibited decreased reflectance in near infrared regions in relation to agriculture and savannah-grassland areas (Ustin and Gamon 2010).

Reflectance declines in the mid infrared regions of the wavelength spectrum are believed to be associated with increased water stress levels, which may be influenced by individual plant structure and leaf morphological characteristics (Santos *et al.* 2010). For example, in the regions ranging from 1.1927-1.3122 μm, previous research revealed reflectance declines with *Pinus* spp. displaying visual symptoms of vegetation stress (Santos *et al.* 2010). Rosso *et al.* (2005) also observed reflectance declines in the near infrared regions in correlation to increased levels of vegetation stress levels, possibly attributed to influences of electromagnetic energy characteristics resulting from decreased intercellular space. Additionally, beyond 1.500 μm, reflectance of vegetation is chiefly attributed the ability of H_20 to absorb electromagnetic radiation (Ustin and Gamon 2010). Moreover, several *Pinus* spp. illustrated a drop in reflectance due to

absorption of water at 1.500 μm, followed by increased reflectance in mid infrared ranging from 1.550 to 1.750 μm, in relation to stress and mortality (Santos *et al.* 2010). Also illustrated by Santos *et al.* 2010, was the effect of bare soil, uncovered by canopy openings due maturing forest growth, indicated by increased reflectance values as well as the variability among soil types to influence reflectance patterns in the mid infrared regions (Santos *et al.* 2010). Spectral properties of soil have been shown to be distinct from plant material (Ustin and Gamon 2010). For example, research centered at Jasper Ridge Biological preserve located in Stanford California, illustrated soil reflectance to be characterized by a slightly increasing slope of a line persisting beyond the visible spectrum and into the near infrared up to approximately 1.800 μm, followed by steady declines leading towards 2.500 μm (Ustin and Gamon 2010).

In the mid infrared portion of the wavelength spectrum ranging from 1.8151 and 1.9471 μm, increased levels of reflectance have been observed as well as declining absorbance in the water absorption band region proximate to 1.900 μm, in areas consisting mostly of non-living *Pinus* spp. (Santos *et al.* 2010). This result may be attributed to possible litter and soil coverage, dehydration of plant structures, and falling of needles (Santos *et al.* 2010). Chemicals involved in the makeup of plants can also influence vegetation reflectance measurements (Ustin and Gamon 2010). For example, the absorption of cellulose in the wavelength spectrum ranging from 2.000 to 2.200 μm has been observed for water limited grass greenery and (coast redwood) *S. sempervirens* needles (Ustin and Gamon 2010).

Located in both near infrared and mid infrared regions of the wavelength spectrum are areas of decreased reflectance located near 0.970, 1.200, 1.450, 1.950 and

2.250 μm and are known as water absorption bands (Sims and Gamon 2003). Field based reflectance measurements demonstrated water absorption bands of the wavelength spectrum ranging from 0.950 to 0.970 μm, 1.150 to 1.260 μm, and 1.520 to 1.540 μm, to be most applicable to water content detection in canopies (Sims and Gamon 2003). In contrast, research has discovered by way of satellite derived indices, utilization of the near IR and mid infrared regions and more specifically, water absorption bands ranging from 0.950 to .970 μm, 1.150 to 1.260 μm, and 1.520 to 1.540 μm, to be highly effective in assessment of water content in canopies in relation to visible and initial near infrared regions (Sims and Gamon 2003). This is because these wavelengths are able to absorbed further into the canopy structure, providing a larger more accurate representation of water content in comparison to the visible region, due to increased reflectance (Sims and Gamon 2003). However, the entire canopy composition as well as individual leaf materials involved may also influence reflectance results in determining canopy water content (Sims and Gamon 2003). This is because as the cross sectional area of leaf materials increase, sensors lose ability to infiltrate further, meaning detection of water would result from narrower and slighter materials, leading to decreased ability to gain a full representation water content in canopies (Sims and Gamon 2003). In certain water band regions, it was determined that the water content of canopy stem structure had less impact on reflectance relative to green tissues (Sims and Gamon 2003). Also, considered in these indices, gaps in the canopy, exposing possible water areas such as small streams or pools, may lead to further errors (Sims and Gamon 2003).

Normalized Difference Vegetation Index (NDVI)

The Normalized Difference Vegetation Index (NDVI) has been well established and utilized by researchers (Filella *et al.* 2004), and is considered a measurement of vegetation greenness (Veraverbeke *et al.* 2010). NDVI has the ability to accurately utilize specific band regions of the wavelength spectrum involved with vegetation physiological characteristics (Pettorelli *et al.* 2005). More centrally, relying on links between increased absorption in the red visible region and higher chlorophyll content (Lichtenhaler *et al.* 1998), as well as increased absorption in near infrared region, the NDVI illustrates a decreased ability of vegetation to reflect heat, denoting vegetation stress (Guerschman *et al.* 2003). NDVI has been shown to have vegetation values spanning above zero to one (Pettorelli *et al.* 2005), and can be broadly viewed with the equation (Near infrared – Red visible region / Near infrared + Red visible region) (Filella *et al.* 2004), with red visible region ranging from 0.63 to 0.69 μm and near infrared region ranging from 0.75 to 0.80 μm (Tucker 1979). Previous research has demonstrated variances in average NDVI values among different cover categories (Yilmaz *et al.* 2008). For example, results indicated that land designated for crops show the largest NDVI values, followed by forest types such as evergreen and riparian woodlands, with lowest average NDVI values indicated for shrub and grassland categories (Yilmaz *et al.* 2008). Additionally, NDVI has also been shown to be successful in cover class determination and can be attributed to the strong relationships among diverse plant assemblages and pigment absorption through the process of photosynthesis (Ustin and Gamon 2010). This enables researchers to strive to obtain the most comprehensive land type classifications.

However, many limitations exist and include discrepancies between field and satellite classifications, errors associated with regions located on the pixel edges, differences in sensor architecture and correction adjustment factors, and variations in approaches and procedures (Ustin and Gamon 2010).

Moreover, NDVI has shown correlations between vegetation water stress and variations in leaf angles in latent phases of previous research involving plant stress in relation to daily vegetation cycles (Dobrowski *et al.* 2005). However, plant physiological changes involved with plant stress have been demonstrated to occur over larger temporal scales (Dobrowski *et al.* 2005). Also, the amount of ground cover has been shown to be directly proportional to NDVI values (van Leeuwen *et al.* 2010). More specifically, even though wavelengths properties of different vegetation types and soil can influence results, elevated NDVI values have been related to increased abundance in cover vegetation (van Leeuwen *et al.* 2010). Attempts have been made to discover new indices with increased accuracy in areas such as plant pathology, early onset of vegetation stress, and mortality (Lichtenhaler *et al.* 1998).

Normalized Burn Ratio (NBR)

Burn severity can be described as the amount of change inflicted by fire disturbance on a particular area (Epting *et al.* 2005). Fire disturbance has been shown to affect vegetation in numerous way including the decreased water content and health, changes in soil properties, density, species types, and arrangements (Soverel *et al.* 2010). In the near infrared and mid infrared regions of wavelength spectrum, changes linked to wild-land fire can be observed using Landsat Enhanced Thematic Mapper Plus (ETM+)

and previous counterpart Landsat Thematic Mapper (TM) (Soverel *et al.* 2010). More specifically, wild-land fire dynamics have been associated with the Landsat image band regions (B4) ranging from 0.76 to 0.90 μm and (B7) ranging from 2.08 to 2.35 μm (Soverel *et al.* 2010). NBR index is composed of bands (B4-B7) / (B4+B7) (Smith *et al.* 2007; Key and Benson 2006) and has been shown to be connected to moisture levels of vegetation (Veraverbeke *et al.* 2010). In post-wild-land fire landscapes, reflectance in the near infrared region and more specifically band 4, has been shown to be lower, while in contrast, mid infrared regions associated with band 7, has been shown to have the largest reflectance escalations (van Wagtendonk *et al.* 2004). Delta NBR results from subtraction of pre- and post-wild-land fire NBR values, then multiplied by a 1000 (Smith *et al.* 2007; Key and Benson 2006), with known values spanning from -1 to 1 (Miller and Thode 2007). Positive delta NBR values indicate decreased amounts of vegetation, while, negative NBR values indicate increased vegetation growth between image acquisition dates, thus designating levels of burn severity and re-growth (Miller and Thode 2007).

Fire managers and researchers alike may potentially benefit from improved accuracy of burn severity analyses in affected areas, temporal analysis of burn severity patterns, and studies involving determination of total carbon emissions (Soverel *et al.* 2010). However, drawbacks and limitations associated with landscape variations have been noted (Miller and Thode 2007). More specifically, there exists the possibility that two distinct high and low areas of vegetation abundance might observe similar pre-and post-NBR, and delta NBR values, resulting in further categorization errors (Miller and Thode 2007). This may occur because NBR lacks the ability to account for vegetation diversity, actual plant material amounts, density and plant cover areas, and may only

relate to vegetation changes between pre- and post-wild-land fire image acquisition dates (Miller and Thode 2007). Nevertheless, the NBR has been elevated in status as the premier index for evaluations of burn severity levels and may be a valuable tool in management strategies following fire disturbance (Veraverbeke *et al.* 2010).

Objectives and Significance

The broad objective of this study was to increase knowledge and explore wild-land fire influences and relationships using available remotes sensing techniques, in an attempt to fill in an existing gap between ecologists and remote sensing (Roughgarden *et al.* 1991). With development of remote sensing technologies, this study's approach in utilization of remote techniques may provide future credible choices to previously established field methods and protocols (Rosso *et al.* 2005). In addition to uncovering important interpretations and trends, remote sensing may add to existing knowledge of fire disturbances. This knowledge is considered essential in allowing leaders to implement wild-land fire policies with an increased awareness of possibilities associated with future fire scenarios (Skinner and Chang 1996).

In an effort to visually interpret landscape change, remote sensing techniques including multi-temporal imagery and NDVI grey-scale imagery were incorporated into this study to gain a more diverse perspective of pre- and post-wild-land fire landscapes (Horning *et al.* 2010). The significance of both techniques can be attributed to technological advances in the last decade having allowed the use of visual interpretation and analysis of remote sensing imagery to be a quick and accessible tool for researchers, forest officials, and fire related agencies to access affected areas (Horning *et al.* 2010).

The utility of this underestimated tool has been linked to the physiology of the human brain, with our increased efficiency to accurately identify, compare, and process significant volumes of landscape change associated visual imagery information, in comparison to recent versions of complex computer programs and algorithms (Horning *et al.* 2010).

A 12-year comparison of NDVI and local meteorological data was performed to observe pre- and post-wild-land fire established trends (van Leeuwen *et al.* 2010). The objective for this pre-fire NDVI time based collection of data was to observe and effectively gather baseline readings for comparisons as well as analysis of decreased NDVI values, which may be linked to fire disturbance (van Leeuwen *et al.* 2010; Vicente-Serrano *et al.* 2011), while also gaining a better understanding of possible relationships which may indirectly influence NDVI values, such as lack of precipitation and drought, abnormal minimum and maximum temperatures (Gomez-Mendoza *et al.* 2008; van Leeuwen *et al.* 2010). Further objectives included collection and utilization of post-wild-land fire NDVI values for comparison and contrast of both complexes vegetation recovery, associated time periods, and related trends (van Leeuwen *et al.* 2010). The significance of this time based approach resides not only in the capacity to establish trends between NDVI, meteorological data, and wild-land fire, but also in the utility of these data to be used in other potential ways including analysis of high and low period durations, ability to connect results to exact time periods, and examination of increased and decreased NDVI intervals (Pettorelli *et al.* 2005). Ustin and Gamon also noted the potential of time based remote sensing technology aiding in an increased

understanding of vegetation cover classification, related to abilities in monitoring phenological tendencies associated with seasonality (Ustin and Gamon 2010).

Although previous studies have used the Composite Burn Index (CBI) for accuracy assessment and validation (Holden *et al.* 2010; Veraverbeke *et al.* 2010), a different approach for statistical analysis was taken using coefficients of determination R^2 correlations between satellite to ground based NDVI values for Butte Humboldt Complex (BHC), Butte Lightning Complex (BLC), and Richardson Springs subplots (MS Excel 2010). Based on previous monitoring abilities of ground based NDVI assessment on post-wild-land fire recovery patterns in 1994 (Filella *et al.* 2004), low to medium correlations of comparisons are expected. Also, NDVI has been shown be effective in shrubland communities, for detection of vegetation responses related to drought influences as well as monitoring vegetation development (Filella *et al.* 2004).

Collection of pre-, post-NBR, and delta NBR data from original BHC and BLC subplots allowed for quantitative and applicable assessment of burn severity levels (van Wagtendonk *et al.* 2004). Low fire severity for savannah grassland type ecosystems have been reported, with observed fire behavior to be rapidly sweeping in nature, however, differences still exist among severity levels between savannah and chaparral communities, both of which encompass BHC affected areas (Skinner and Chang 1996). Nevertheless, a low burn severity levels are expected for BHC, with increasing burn severity levels expected for BLC.

CHAPTER III

METHODS

Study Locations

In June 2008, two wild-land fires consumed large areas of natural and wooded landscapes in rural Butte County, California (Calfire 2010). June 11, 12:13pm, near Humboldt Road in Stillson Canyon, the Butte Humboldt Complex first appeared when an initial fire broke out and then spread rapidly to over 23,344 acres causing the destruction of 87 homes, ten injuries, and 20.5 million dollars in damages (Calfire 2010). Ten days later, on June 21, 2008, 2:00 PM, while local fire crews were still dealing with the aftermath caused by the Butte Humboldt Complex, the Butte Lightning Complex first appeared with initial fires racing through areas near Concow and Highway 70, spreading to over 59,440 acres, causing the destruction of 106 homes, 71 injuries, and 85.3 million dollars in damages (Calfire 2010)

In an effort to gain a unique qualitative (visual) sense of magnitude and impact of wild-land fires on vegetation and associated landscape change, as well as to properly designate “unburned,” “burned edge,” “burned center,” and “reference” subplot locations, entire areas affected by the Butte Humboldt and Lightning Complexes were examined via satellite remote sensing Landsat 5 imagery and Envi 4.8 analysis software (USGS 2010; Envi 4.8 2010). Additionally, five miles northeast of Chico, California, at a location named Richardson Springs, a third set of subplots were selected to be used as

control for comparison of satellite to ground based methods. Selection of Richardson Springs was made due to the lack of fire disturbance in the last twelve years, associated fire suppression efforts, and close proximity to the Butte Humboldt Complex subplot locations (Calfire 2010).

Based on this close proximity between Butte Humboldt Complex and Richardson Springs lower elevation subplots, less than ten miles apart, both surrounding landscapes share similar vegetation types and compositions (Barbour *et al.* 1993). Within this elevation region (below 600 ft.), savannah type grasslands persist with a mosaic of sparsely spatially oriented large oaks (*P. santrons*), foothill pine (*Pinus sabiniana*), and California Buckeye *(Aesculus californica*) (Barbour *et al.* 1993). Showering the landscape, an understory of herbaceous shrubs and herbs are present and include Christmas berry (*Heteromeles arbutifolia*), California coffeeberry (*Rhamnus californica*), fescue bunchgrasses (*F. occidentalis, Festuca californica*), and hedge nettle (*Stachys rigida*) (Barbour *et al.* 1993). Also contributing to species diversity other species of vegetation include squaw bush (*Rhus trilobata*), Red bud (*Cercis occidentalis*), and Chinese house (*Collinsia* spp.) (Barbour *et al.* 1993). As elevation increases toward the east in areas affected by the Butte Humboldt Complex, the landscape transitions into chaparral type vegetation that include Manzanita (*Arctostaphylos sp.*), Scrub oak (*Quercus dumosa*), and chamise (*Adenostoma fasciculatum*) (Barbour *et al.* 1993). In contrast, areas affected by the Butte County Lightning Complex were at an overall higher elevation and located on the eastern side of the Sierra Nevada Mountain Range in Plumas National Forest (Barbour and Major 1977). This mixed conifer forest has dense softwood vegetation that include Jeffrey pine (*Pinus jeffreyi*), Ponderosa pine (*Pinus ponderosa*),

and Incense cedar (*Calocedrus decurrens*) along with an understory of shrubs consisting of Greenleaf Manzanita (*Arctostaphylos patula*), Squaw Carpet (*Ceanothus prostratus*), and Rabittbush Goldenweed (*Haplopappus bloomeri*) (Barbour and Major 1977).

Satellite Remote Sensing Imagery

In an effort to visually determine varying levels of landscape change, magnitude and direction of affected areas, multi-temporal false color RGB images were constructed using Landsat 5 images, WRS path 44 row 32 and Envi 4.8 computer software (USGS 2010; Envi 4.8 2010). Two time comparisons featuring seven year pre wild-land fire and one year pre- and post-wild-land fire were selected for both Butte Humboldt and Lightning Complexes. Starting with the longer time period of seven year pre wild-land fire, multi-temporal false color images for both complexes were constructed by shifting the red monitor pixels to become the most recent entire Landsat 5 image taken on 04/02/2008, then shifting both green and blue monitor pixels further back in time to the entire Landsat 5 image taken on 04/28/2000 (USGS 2010; Envi 4.8 2010; Horning *et al.* 2010). Next, the same methods were repeated for one year pre- and post-wild-land fires with Landsat 5 images taken on 04/05/2009 and 04/02/2008, respectively (USGS 2010; Envi 4.8 2010; Horning *et al.* 2010). Burned center two subplot coordinates (Appendix A) for each complex were selected to give an overall uniform orientation of images for visual analysis. A zoom magnification factor of two was utilized, with an estimated coverage distance of over twenty miles between vertical and horizontal borders (Envi 4.8 2010).

Selection of subplot locations involved the use of post-fire images for both Butte Humboldt and Lightning Complexes. Based on the observable burn scars, subplot locations were determined. Each subplot was given labels that correspond to its location in relation to the fire disturbances. For both Complexes, three subplots were designated "burned center," three subplots were designated "unburned," three subplots were designated "burned-edge," and one subplot was designated as "reference," totaling ten subplots per fire. An additional ten subplots were selected for Richardson Springs and labeled Richardson Springs (control).

Time-based data imagery was acquired by downloading eighty five available Landsat 5 images for spring and summer months dating back twelve years from USGS Landsat data archives WRS path 44, Row 32 (USGS 2010). Spectral analysis was performed using Envi 4.8 computer software for each of the 30 total designated subplots, with NDVI values recorded for the months of April, May, June, July, and August, starting with April 2010 and spanning back 12 years to April 1998 (Envi 4.8 2010). April through August months were selected for the NDVI temporal based data analysis in an effort to minimize phenological vegetation differences occurring throughout yearly summer-winter vegetation cycles, as well as achieving the optimal time frame for studying Butte Humboldt and Lightning Complexes pre- and post-wild-land fire vegetation responses and recovery (Paruelo and Lauenroth 1995; Guerschman *et al.* 2003). Also, the time intervals associated with these wild-land fires made for ideal spectral measurement properties associated with peak vegetation growth (Horning *et al.* 2010). Other benefits included reduced cloud cover and rainfall amounts in relation to winter months and ideal crowning vegetation growth (Horning *et al.* 2010). The onsets of

both wild-land fires occurring in early spring-summer in conjunction with related seasonality contributed to the improved accuracy of noted results (Horning *et al.* 2010). The NDVI values were recorded at each subplot location with an individual pixel size of 30 by 30 meters (Envi 4.8 2010). Using Landsat 5 imagery and Envi software analysis with a 30 by 30 meter pixel size was ideal for overall spatial resolution because of the vast areas associated with wild-land fire (USGS 2010; Envi 4.8 2010; Horning *et al.* 2010).

Time based NDVI data for both Butte Humboldt and Lighting Complexes were compared to the nearest local meteorological data available in an attempt to advance insight into climate influences on wild-land fires (NOAA 2010). Maximum and minimum temperatures, and precipitation amounts for each individual day of the month, April through August, from 1998 through 2010, were initially downloaded and printed from NOAA website for Paradise weather station (NOAA 2010). Twelve-year time based meteorological data was then used to construct an appropriate scale climate graph for comparison.

In addition, to gain further knowledge about levels of burn severity, pre-NBR (Normalized Burn Ratio), post-NBR, and delta-NBR values were calculated for both Butte Humboldt and Lightning Complex original subplots. Based on previous research illustrating the ecological relevance of post-wild-land fire data collection within a year time frame (Soverel *et al.* 2010), Landsat 5 images dated 04/02/2008, 04/05/2009, and 08/14/2010 were selected to perform band-math calculations to collect pre- and post-NBR values, using Envi 4.8 computer software (USGS 2010; Envi 4.8 2010) (Appendix

D). Delta NBR was calculated by subtracting Pre-NBR from post-NBR values (Veraverbeke *et al.* 2010).

Ground Based Remote Sensing Methods

With the use of original satellite subplot coordinates, a total of thirty subplots were identified using a hand held GPS unit (Garmin 2008), on April 19, 21, and 23, 2010. A total of ten individual reflectance scans per subplot were collected using a Unispec SC portable spectrometer (Unispec SC, PP systems 2008) (Appendix B). The objective of this field sampling process was to stay within the 30 by 30 meter barriers, while also striving for an even and broad distribution of individual scan locations within each subplot, in an effort to gain a uniform composite of the landscape. At each subplot location, reflectance measurements were taken at a distance of approximately two meters from the ground, with the optic sensor held slightly offset and angularly away, in a vertical out-stretched arm, while standing to insure the least possible interference due to human appendages, such as feet, and also to gain fair representation vegetation diversity. At this height, the Unispec SC portable spectrometer scans the landscape in a helical cone shape becoming larger as height is increased, with a measured circular pattern of 4 m^2 (Unispec SC, PP systems 2008). Each individual scan provided an individual complete spectral signature ranging from 310 to 1100 nm, in 10nm increments (Unispec SC, PP systems 2008). Following field spectrometer instructions and protocol (Appendix B), a white reflectance board was used to minimize differences in light versus cloudy conditions between scan which enabled calibration by means of reference (Unispec SC, PP systems 2008; Letts *et al.* 2008). Other factors, such as possible device noise, were

reduced by applying dark scans prior to data collection, to achieve increased accuracy in results (Unispec SC, PP systems 2008; Letts *et al.* 2008). Reflectance values for each wavelength increment across the spectrum were calculated for each subplot by dividing the subplot data by reference white board data, with averages for each subplot used to derive NDVI values (Unispec SC, PP systems 2008).

CHAPTER IV

RESULTS

Multi-temporal Imagery

It is believed the color red, shade, and intensity may represent negative ecosystem impacts, such as deforestation from logging as well as other possible disturbances, while in contrast, blue, shade, and intensity may denote new vegetation growth (Horning *et al.* 2010). In an effort to identify fire disturbance impacts and landscape change, while using above premise to guide interpretation, analysis of BHC and BLC multi-temporal images yielded insightful visual results (Horning *et al.* 2010). Multi-temporal Landsat 5 images of the areas affected by Butte Humboldt Complex were visually assessed using band five (1.55-1.75 μm): R (04/02/2008), G (04/28/2000), B (04/28/2000) spanning over a seven-year period prior to the wild-land fire and band five (1.55-1.75 μm): R (04/05/2009), G (04/02/2008), B (04/02/2008) spanning over a one-year period pre- and post-wild-land fire (Horning *et al.* 2010). Multi- temporal image spanning over seven years prior to the wild-land fire showed a light red hue over the entire region (Figure 1). In contrast, the multi-temporal image spanning over a year pre- and post-wild-land fire showed a light blue hue with regions of slightly lighter shades of blue present (Figure 1) Both color composites indicated noticeable levels of landscape change (Horning *et al.* 2010).

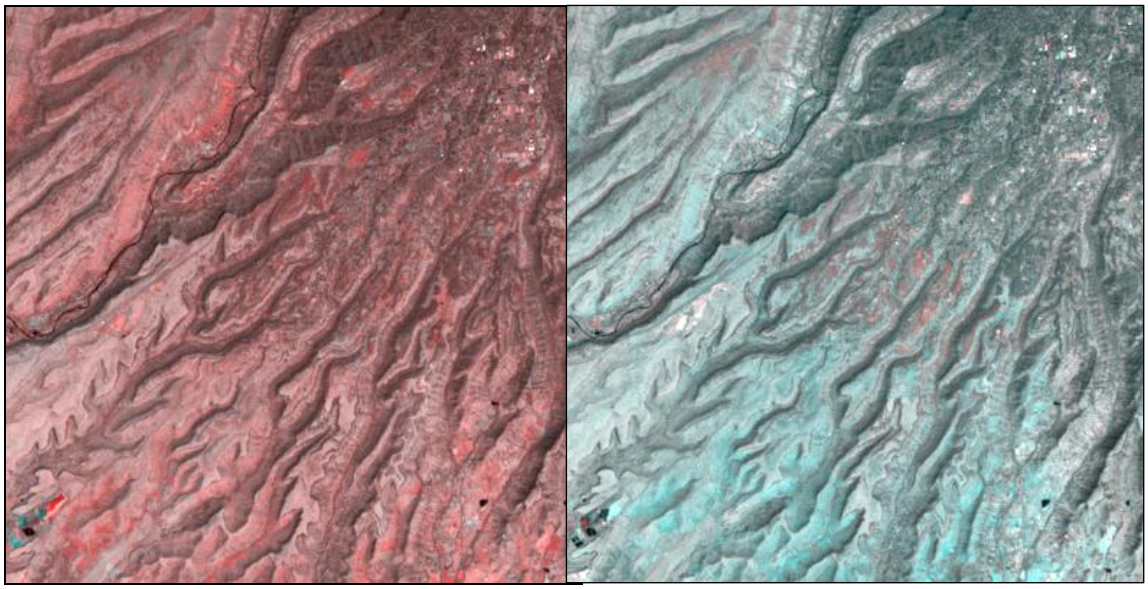

Fig. 1. Multi-temporal images of Butte Humboldt Complex, band five: (left) R (04/02/2008), G (04/28/2000), B (04/28/2000), (right) R (04/05/2009), G (04/02/2008), B (04/02/2008) (Landsat 5 images, thor atomspherically corrected, WRS path 44, row 32) (USGS 2010; Envi 4.8 2010).

Multi-temporal Landsat 5 images of the areas affected by Butte Lightning Complex were also visually assessed using band five (1.55-1.75 μm): R (04/02/2008), G (04/28/2000), B (04/28/2000) spanning over a seven-year period prior to the wild-land fire, and band five (1.55-1.75 μm): R (04/05/2009), G (04/02/2008), B (04/02/2008) spanning over a one-year period pre- and post-wild-land fire (Figure 2) (Horning *et al.* 2010). Multi- temporal image spanning over seven years prior to the wild-land fire showed both dark red and deep bright blue regions, while in contrast, the multi-temporal image spanning over a year pre- and post-wild-land fire showed affected areas in bright intense red (Figure 2). Both color composites indicated noticeable levels of landscape change (Horning *et al.* 2010).

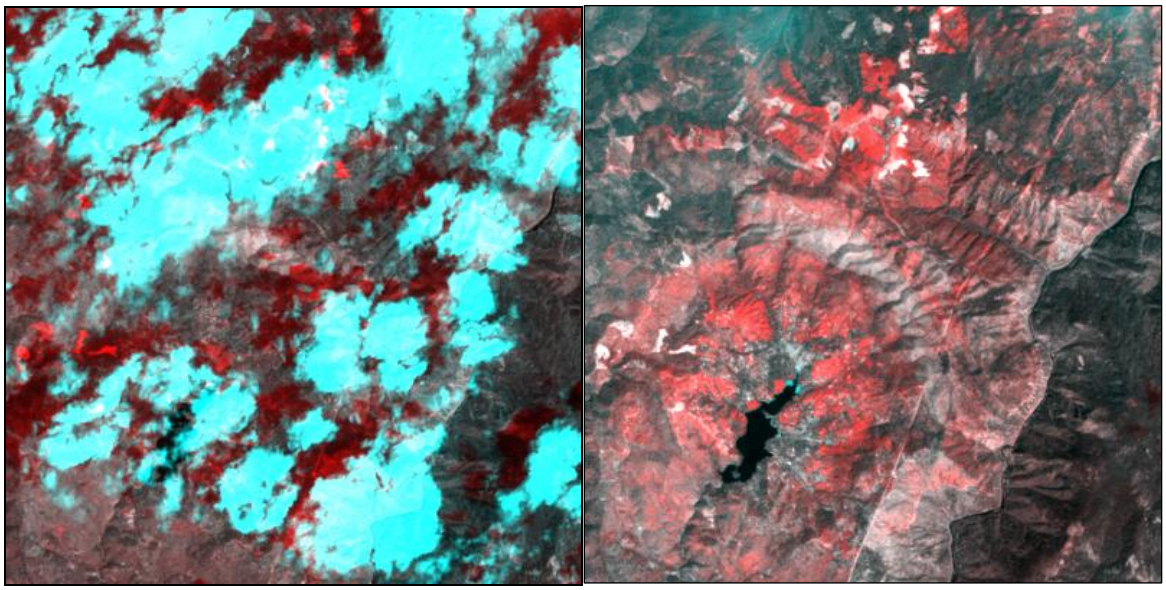

Fig. 2. Multi-temporal images of Butte Lightning Complex, band five: (left) R (04/02/2008), G (04/28/2000), B (04/28/2000), (right) R (04/05/2009), G (04/02/2008), B (04/02/2008) (Landsat 5 images, thor atomspherically corrected, WRS path 44, row 32) (USGS 2010; Envi 4.8 2010).

Landsat 5 Normalized Difference Vegetation Index (NDVI) grey-scale images of pre- (04/02/2008) and post- (04/05/2009) Butte Humboldt Complex were visually assessed. The pre-wild-land fire NDVI grey scale image showed the presence of healthy vegetation with little or no destruction (Figure 3) (Horning *et al.* 2010). In contrast, the post-wild-land fire image clearly showed visible signs of destruction illustrated by the magnitude and direction of the subsequent burn scar (Figure 3).

Landsat 5 NDVI grey-scale images of pre- (04/02/2008) and post- (04/05/2009) Butte Lightning Complex were visually assessed. The pre-wild-land fire NDVI grey-scale image showed the presence of healthy vegetation with a slight semi-circular ring of destruction in the upper center area (Figure 4) (Horning *et al.* 2010). In

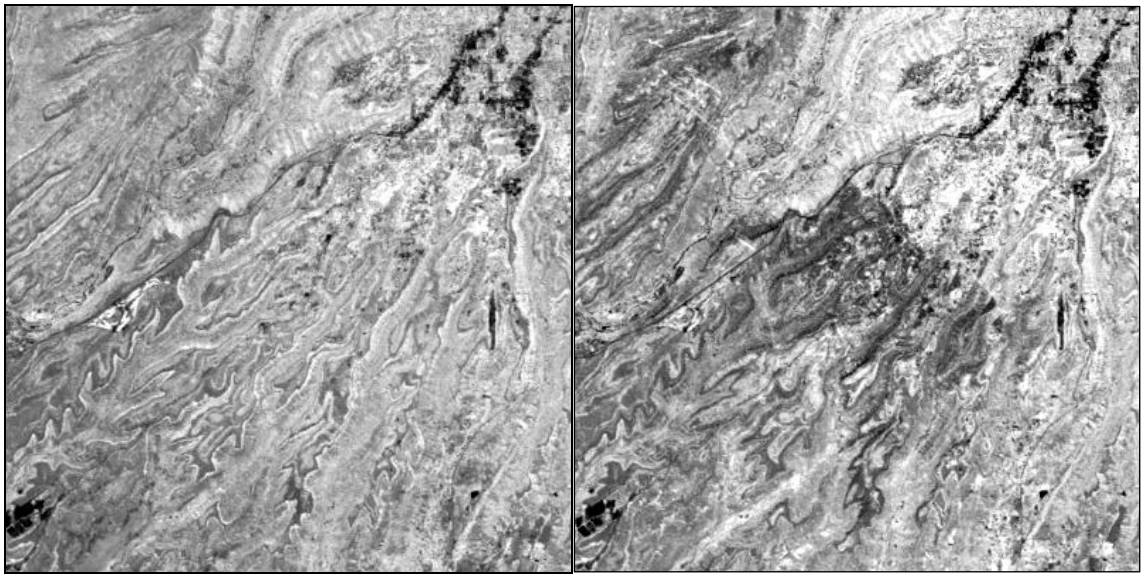

Fig. 3. NDVI pre- and post-wild-land fire grey-scale images of BHC (left) (04/02/2008) and (right) (04/05/2009) (Landsat 5 images, thor atomspherically corrected, WRS path 44, row 32) (USGS 2010; Envi 4.8 2010).

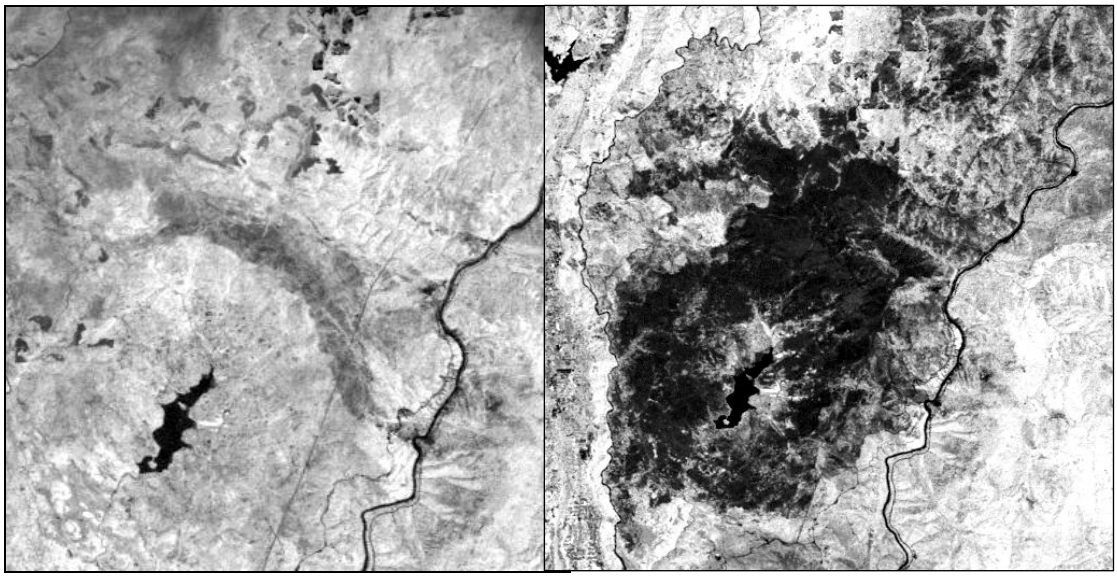

Fig. 4. NDVI pre- and post-wild-land fire grey-scale images of BLC (left) (04/02/2008) and (right) (04/05/2009) (Landsat 5 images, thor atomspherically corrected, WRS path 44, row 32) (USGS 2010; Envi 4.8 2010).

contrast, the post-wild-land fire image clearly showed visible signs of sizable destruction illustrated by the magnitude and direction of the subsequent burn scar (Figure 4).

Analysis of Time Based NDVI with Local Meteorological Data

Analysis of Normalized Difference Vegetation Index (NDVI) for Butte Humboldt Complex reference and unburned subplots, April thru August, over a twelve-year span, showed temporal oscillation patterns with unburned subplot number three, consisting of the highest overall NDVI values followed by unburned one subplot, reference subplot, and unburned two subplot. Unburned three subplot NDVI values decreased to no data from 7/7/2008 to 8/8/2008, followed by a sharp increase, with the highest NDVI value for this increase occurring on 5/7/2009, and a slightly lower than the previous NDVI oscillation pattern observed thereafter. Unburned two followed a similar trend with the lowest NDVI values overall recorded on 7/7/2008 and 7/23/2008. Also, for unburned two subplot, there was a sharp increase in NDVI values on 6/5/2002 followed by a decrease to no data from 6/21/2002 to 8/24/2002 (Figure 5a). A decrease in NDVI values was also observed for both unburned two and reference subplots on 8/22/2007. Unburned one subplot maintained temporal oscillation patterns throughout the entire time duration (Figure 5a).

Analysis of NDVI for Butte Humboldt Complex reference and burned edge subplots, April thru August, over a twelve-year span, showed temporal oscillation patterns, with burned edge one and two subplots showing the highest overall NDVI values followed by reference and burned edge three subplots. Burned edge three subplot decreased to no data from 7/7/2008 to 7/23/2008 followed by a sharp increase in NDVI

(a)

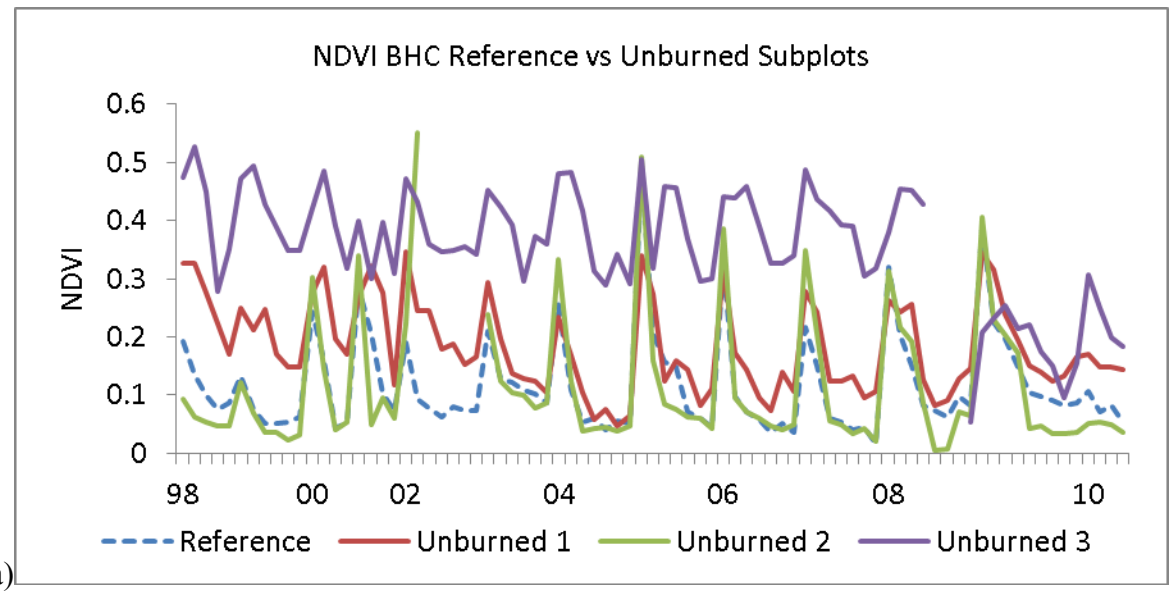

(b)

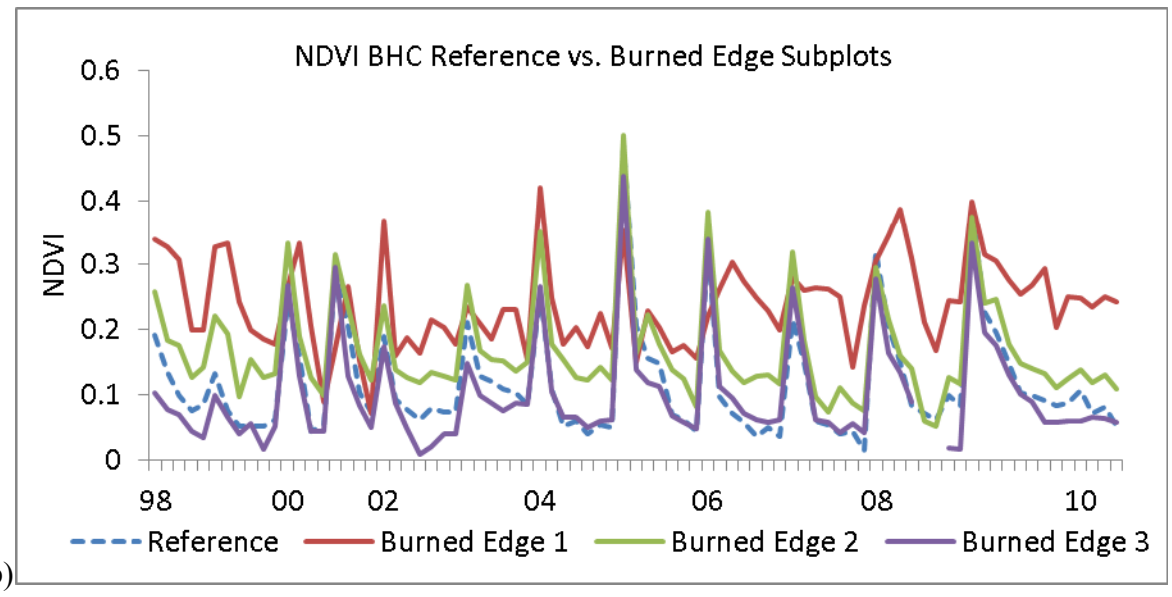

(c)

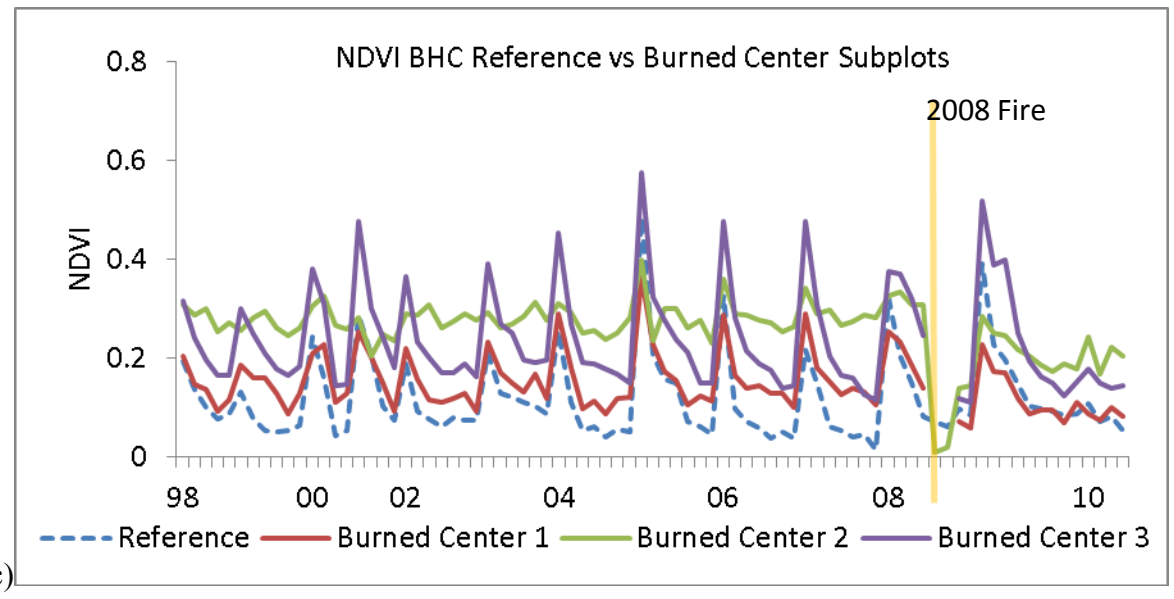

(d)

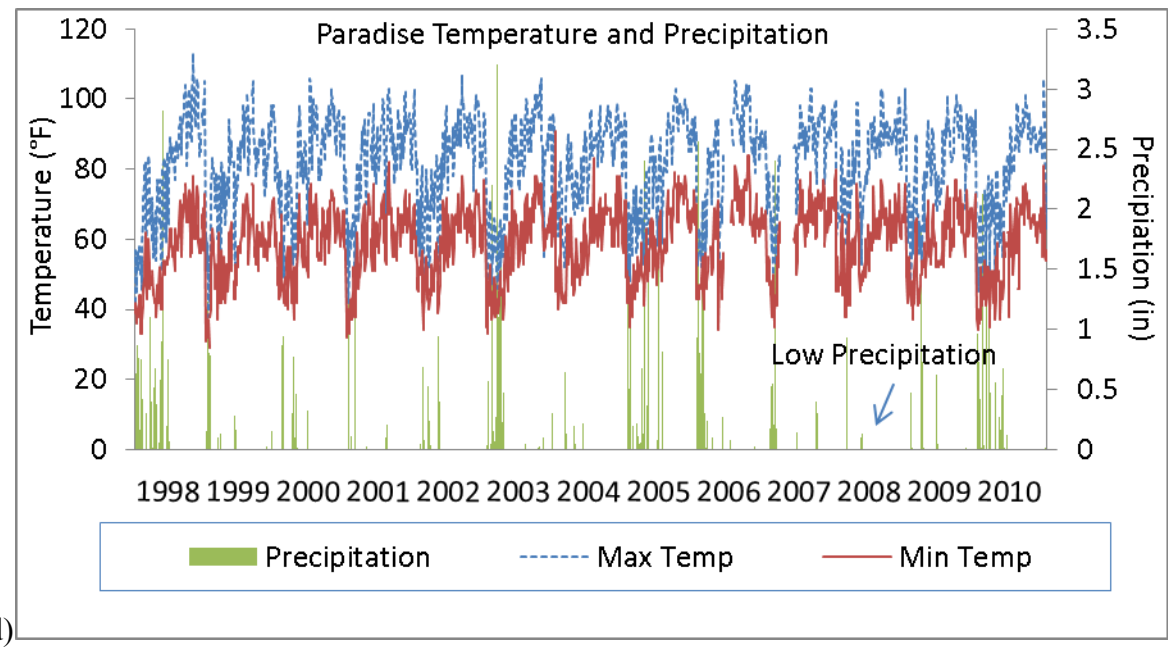

Fig. 5. Twelve year time based NDVI data, April through August (1998-2010). (a) BHC reference and unburned subplots, (b) reference and burned edge subplots, (c) reference and burned center subplots, (d) Paradise weather station twelve year time based percipitation and temperature data, with minimium and maximium temperatures, April through August (1998-2010). (Data from NOAA 2010)

values with the highest NDVI value for this increase occurring on 4/5/2009. Additionally, burned edge subplot number three showed a decrease in NDVI values relative to the oscillation trends on 7/7/2002 (Figure 5b). Both burned edge two and reference subplots maintained NDVI temporal oscillation patterns throughout the time duration, except for a decrease to near zero for reference subplot occurring on 8/22/2007 (Figure 5b).

Analysis of NDVI for Butte Humboldt Complex reference and burned center subplots, April thru August, over a twelve-year span, showed temporal oscillation patterns, with burned center two and three subplots showing the highest overall NDVI values followed by burned center one and reference subplots. Burned center one and three subplots showed initial decreases in NDVI prior to the Butte Humboldt Complex, then both subplots decreased further to no data from 7/7/2008 to 7/23/2008, followed by a sharp increase in NDVI with the highest NDVI values for these increases occurring on 4/5/2009 (Figure 5c). Burned center two subplot decreased to near zero from 7/7/2008 to 7/23/2008, followed by an increase in NDVI with the highest NDVI value for this increase occurring on 4/5/2009. Reference subplot maintained NDVI temporal oscillation patterns throughout the entire time duration, except for a decrease to near zero occurring on 8/22/2007 (Figure 5c).

Paradise Weather Station temperature data, April thru August, over a twelve-year span, showed oscillation pattern of maximum and minimum variation of temperatures in degrees Fahrenheit (Figure 5d) (NOAA 2011). Precipitation amounts in inches, illustrating periods of drought and rainfall (NOAA 2011). An extended period of drought was observed prior to the onset of Butte Humboldt and Lighting Complexes (Figs 5, 6) (NOAA 2011; Calfire 2010).

Analysis of NDVI for Butte Lightning Complex reference and unburned subplots, April thru August, over a twelve-year span, showed temporal oscillation patterns, with the reference subplot showing the highest overall NDVI values, followed by unburned two, unburned three, and unburned one subplots. Unburned one subplot started the time duration with most NDVI values resulting in above 0.4, and then decreased significantly to below .05 from 5/4/2002 to 8/24/2002, followed by an increase and oscillation pattern not reaching NDVI values above 0.35 (Figure 6a). Unburned two, three, and reference subplots maintained NDVI temporal oscillation patterns throughout the entire time duration except for the reference subplot showing three noticeable decreases in NDVI values on 5/1/2001, 8/11/2003, and 7/23/2008 (Figure 6a).

Analysis of NDVI for Butte Lightning Complex reference and unburned subplots, April thru August, over a twelve-year span, showed temporal oscillation patterns, with burned edge one and two subplots showing the highest overall NDVI values. However, burned edge one subplot showed no data on 4/28/2000 (Figure 6b). Reference and burned edge three subplots both showed lower NDVI values overall with three noticeable decreases (Figure 6b). Decreased NDVI values were observed on 5/1/2001, 8/11/2003, and 7/23/2008 for reference subplot and 4/28/2000, 4/26/2005 and 4/2/2008 for burned edge three subplot (Figure 6b).

Analysis of NDVI for Butte Lightning Complex reference and burned center subplots, April thru August, over a twelve-year span, showed temporal oscillation patterns, with the reference and burned center three subplots showing the highest overall NDVI values, followed by burned center two and one subplots. Burned center one, two, and three subplots showed oscillation patterns with noticeable decreases on 4/28/2000

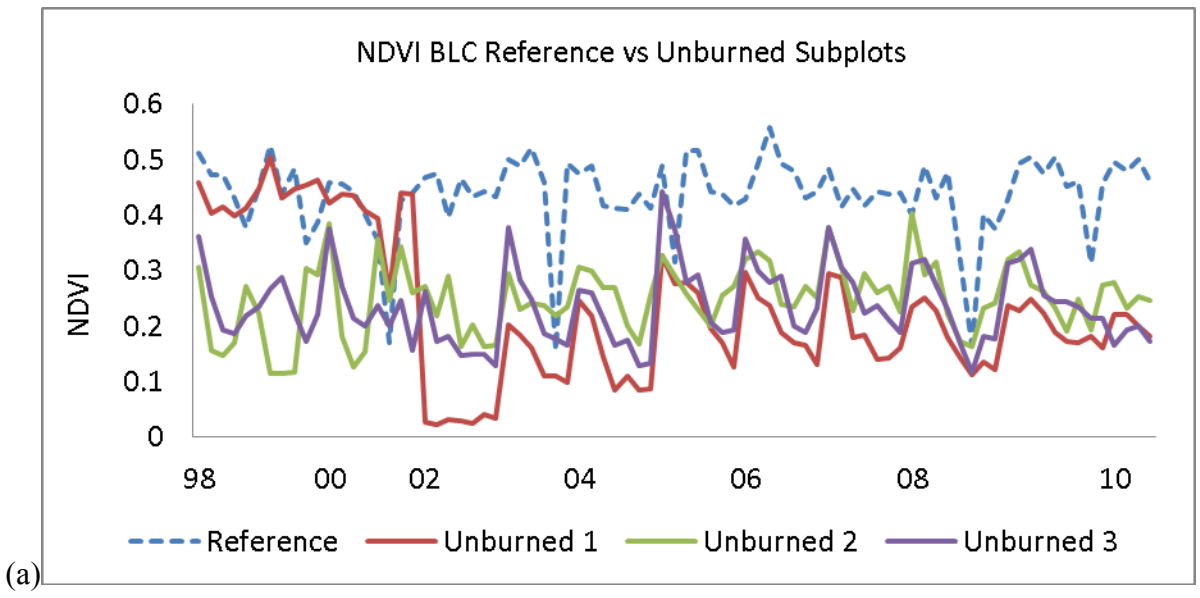

(a)

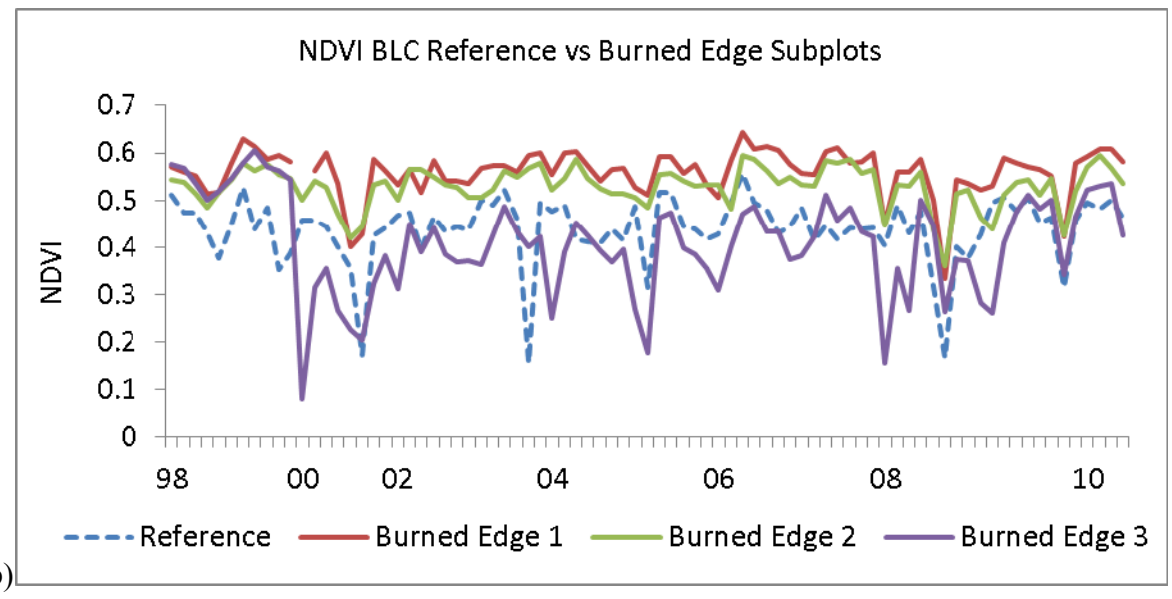

(b)

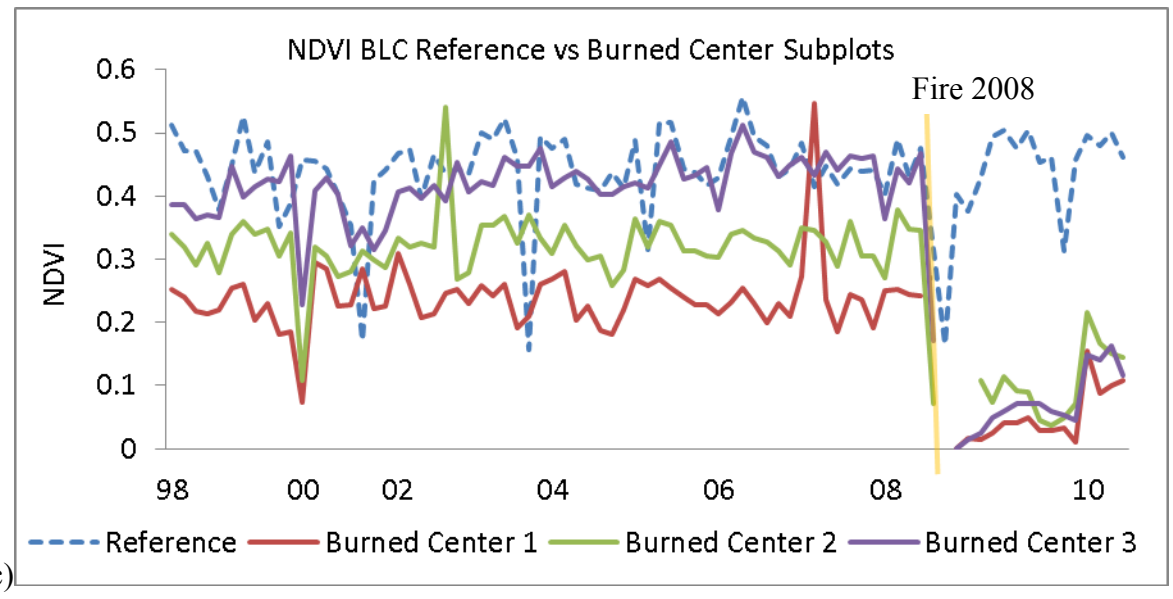

(c)

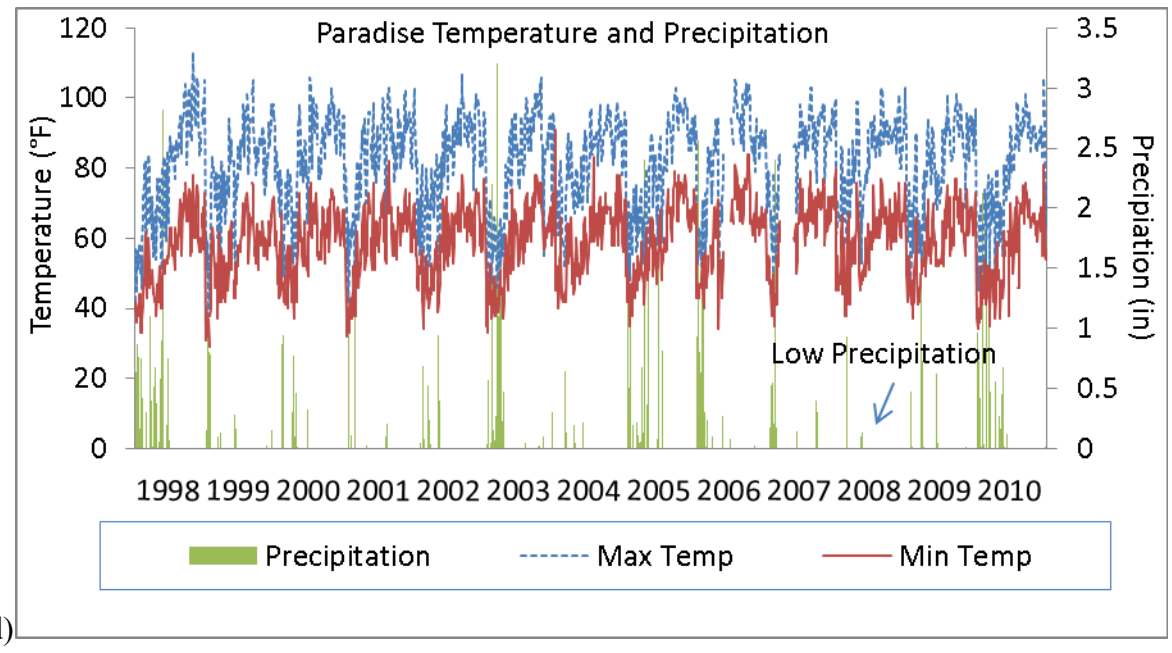

(d)

Fig. 6. BLC 12-year (1998-2010) April through August, NDVI time based data. (a) reference and unburned subplots, (b) reference and burned edge subplots, (c) reference and burned center subplots, (d) 12-year (1998-2010) April through August, time based local meteriological data, minumium and maximium temperatures, and precipitation. (Data from NOAA 2010).

and an increases on 7/23/2002 for burned center two subplot and on 5/18/2007 for burned center one subplot (Figure 6c). Reference subplot showed temporal oscillation patterns throughout the entire time duration except for three noticeable decreases in NDVI values on 5/1/2001, 8/11/2003, and 7/23/2008. Burned center one subplot showed an initial slight decrease in NDVI values from 5/4/2008 to 6/5/2008, then decreasing further to no data from 7/7/2008 to 7/23/2008, with a zero value observed on 8/8/2008 (Figure 6c). Burned center one subplot then showed a slight increase and decrease in NDVI values staying below .05 from 8/24/2008 to 8/27/2009, followed by an increase on 6/27/2010. Burned center two subplot showed an initial slight decrease in NDVI values from 5/4/2008 to 6/5/2008, and then decreased to below an NDVI value of 0.1 on 7/7/2008, followed by a further decrease to no data from 7/23/2008 to 8/24/2008 (Figure 6c). Burned center two subplot then observed a low NDVI value on 4/5/2009, trailed by a small oscillation and decreasing NDVI values incrementally from 4/21/2009 to 7/26/2009, with a subsequent increase in NDVI values recorded from 8/11/2009 to 6/27/2010 (Figure 6c). Burned center three subplot showed an initial slight increase in NDVI values from 5/4/2008 to 6/5/2008, then decreased to below 0.2 on 7/7/2008, followed by a further decrease to no data on 7/23/2008, with a zero value observed on 8/8/2008 (Figure 6c). Burned center three subplot then observed a near zero value on 8/24/2008, followed by a slight increase and decrease in NDVI values staying below .08 from 4/5/2009 to 8/27/2009, followed by an increase on 6/27/2010 (Figure 6c).

Coefficient of Determination R^2 Comparisons Between NDVI Satellite and Ground Based Values

Statistical analysis using Coefficient of Determination R^2 was used to compare Normalized Difference Vegetation Index values from satellite and ground methods of three northern California locations: Butte Humboldt Complex, Butte Lightning Complex, and Richardson Springs (MS Excel 2010). Butte Humboldt Complex and Richardson Springs locations both showed weak positive linear correlations (R^2 = 0.0859) (Figure 7) and (R^2 =0 .3555) (Figure 7) (MS Excel 2010). In contrast, Butte Lightning Complex showed a slightly negative linear correlation of (R^2 = .001) (Figure 7) (MS Excel 2010).

Pre-NBR, Post-NBR, and dNBR Values for Butte Humboldt and Lightning Complex Subplots

The majority of pre- and post-NBR values were within normal ranges and not above or below a value of 1 (Miller and Thode 2007). Exceptions were observed for BLC burned center one subplot with a value of zero and burned center two and three subplots with large post- NBR values (Table. 1). Delta NBR values for BHC unburned three subplot and BLC unburned two and burned center one subplots indicated low to moderate levels of burn severity (Table. 1) (Miller and Thode 2007). In contrast, BHC unburned one and two, and burned edge two subplots indicated a burn severity of unburned (Table. 1) (Miller and Thode 2007). Also, BLC reference, unburned one and three subplots, and all burned edge subplots observed delta NBR values indicating unburned levels of burn severity (Table. 1) (Miller and Thode 2007). Delta NBR values for BHC reference,

(a)

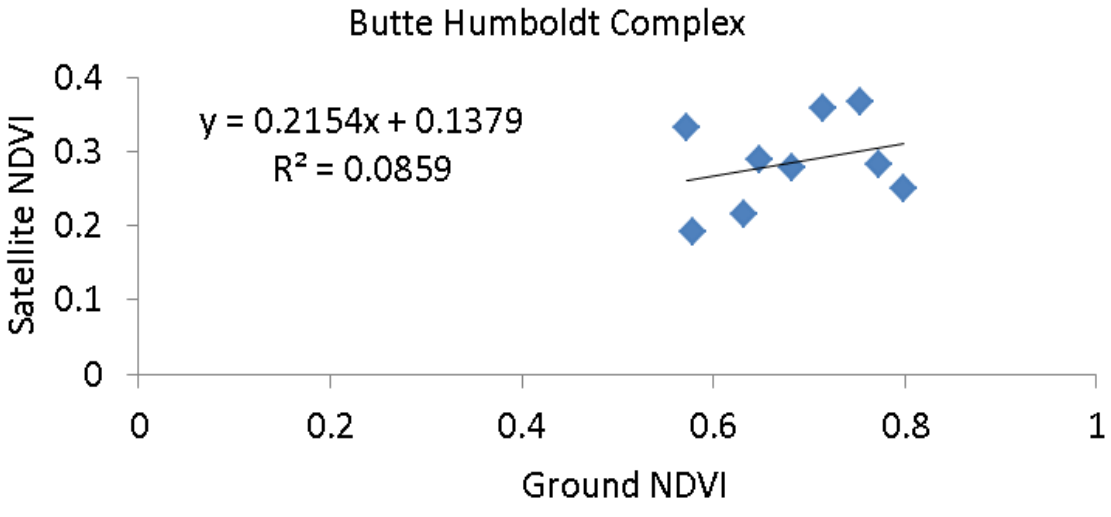

(b)

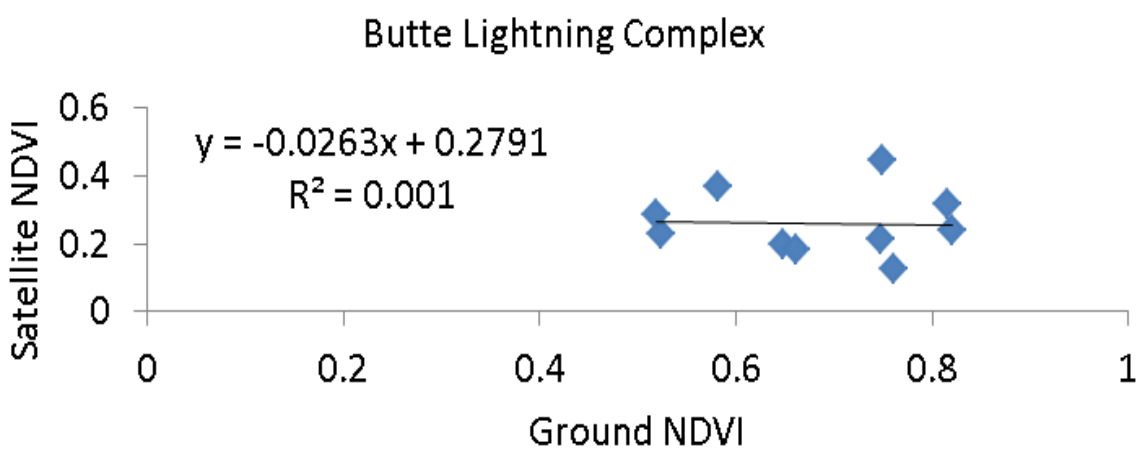

(c)

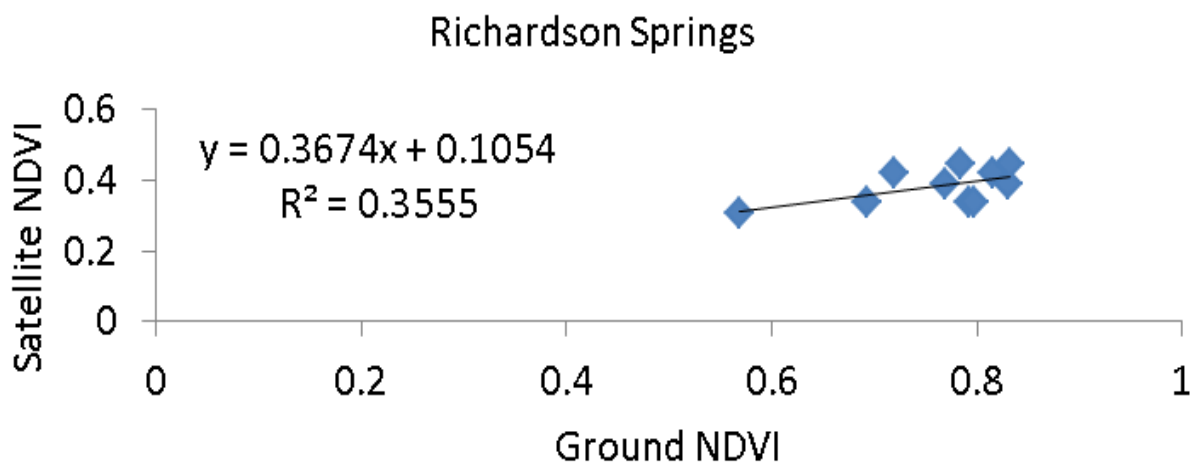

Fig. 7. Comparison of remote sensing satellite to ground based normalized difference vegetation index (NDVI) values by means of Coefficient of Determination R^2 (MS Excel 2010). (a) BHC derived satellite (8/14/2010) versus ground based NDVI (4/16/2011), (b) BLC satellite derived NDVI (8/14/2010) versus ground based NDVI (4/19/2011), (c) Richardson Springs satellite derived NDVI (8/14/2010) versus ground based NDVI (4/21/2011).

burned edge one and three, and burned center three subplots indicated low re-growth (Table. 1) (Miller and Thode 2007). Delta NBR values for BHC burned center one and two subplots indicated low levels of burn severity (Table. 1) (Miller and Thode 2007). Unexpectedly, delta NBR values for burned center subplots two and three were not identifiable (Miller and Thode 2007). However, more recent post-NBR imagery of BLC burned center two and three subplots, yielded values within normal ranges, with delta NBR values indicating low and mid to high burn severity (Table. 1) (Miller and Thode 2007).

Table 1. Pre-Normalized Burn Ratio (NBR), post-Normalized Burn Ratio (NBR), and delta Normalized Burn Ratio (dNBR) values for Butte Humboldt and Lightning Complex subplots

Fire	Sub-Plot Location	Pre-NBR ($_{band}4-_{band}7$)/ ($_{band}4+_{band}7$)	Post-NBR ($_{band}4-_{band}7$)/ ($_{band}4+_{band}7$)	dNBR (Pre-NBR - Post-NBR)	Severity Level
Butte Humboldt Complex	Reference	0.220339	0.327273	-0.106934	Low Regrowth
	Unburned 1	0.350877	0.431193	-0.080316	Unburned
	Unburned 2	0.247525	0.302752	-0.055227	Unburned
	Unburned 3	0.411765	0.044776	0.366989	Low-Moderate
	Burned Edge 1	0.264000	0.385665	-0.121665	Low Regrowth
	Burned Edge 2	0.203540	0.294118	-0.090578	Unburned
	Burned Edge 3	0.169811	0.295238	-0.125427	Low Regrowth
	Burned Center 1	0.203883	0.102041	0.101842	Low
	Burned Center 2	0.368421	0.223529	0.144892	Low
	Burned Center 3	0.339286	0.440678	-0.101392	Low Regrowth
Butte Lightning Complex	Reference	0.494949	0.538462	-0.043513	Unburned
	Unburned 1	0.148515	0.081081	0.067434	Unburned
	Unburned 2	0.400000	0.020354	0.379646	Low-Moderate
	Unburned 3	0.312500	0.264151	0.048349	Unburned
	Burned Edge 1	0.612903	0.645161	-0.032258	Unburned
	Burned Edge 2	0.617647	0.606557	0.011090	Unburned
	Burned Edge 3	0.421687	0.478261	-0.056574	Unburned
	Burned Center 1	0.358025	0.000000	0.358025	Low-Moderate
	Burned Center 2	0.355556	2.702128	-2.346572	N/A
	Burned Center 3	0.489796	2.129630	-1.639834	N/A
	Burned Center 2	0.400000	0.204082	0.195918	Low
	Burned Center 3	0.467890	0.008696	0.459194	Mid-High

CHAPTER V

DISCUSSION

Multi-temporal Imagery

Multi-temporal imagery has shown great potential for assessment of landscape change, however, because of lack of previous research and literature this topic, caution must be stressed in interpretation of results on a singular level, without further comparisons to other types of remote sensing techniques and indices (Horning *et al.* 2010). Recent research concerning multi-temporal imagery has revealed relationships associated with the colors red and blue, shade and intensity, and visual representations of various levels of landscape change (Horning *et al.* 2010). Both multi-temporal images of Butte Humboldt Complex displayed noticeable levels of landscape change (Horning *et al.* 2010). The seven year pre-fire multi- temporal image showed the area of study encompassed in a low intensity red hue (Figure 1), which represents negative landscape change (Horning *et al.* 2010). In contrast, one year pre- and post-wild-land fire multi-temporal image showed the entire area encompassed in a light blue hue (Figure 1), which indicates some form of positive re-growth (Horning *et al.* 2010). This light blue hue associated with positive re-growth may possibly be linked to increased recovery due to the elasticity of species typical of savannah grassland type vegetation in relation to fire disturbance (Hernandez-Clemente *et al.* 2009; Horning *et al.* 2010; Vicente-Serrano *et al.* 2011). Also, results indicated the plausibility of increased levels of negative impact,

visually displayed in light levels of red, shade, and intensity for BHC seven year pre-wild-land fire in relation to one year pre- and post-wild-land fire (Figure 1) and may perhaps be attributed to previously documented fire disturbances in affected areas (Calfire 2010; Horning *et al.* 2010).

Comparison of multi-temporal images in areas affected by the Butte Lightning Complex revealed extensive levels of landscape change (Horning *et al.* 2010). The seven year pre-wild-land fire multi-temporal image showed patchy areas of deep blue and deep red (Figure 3), which may indicate noticeable levels of both positive and negative landscape change (Horning *et al.* 2010). In contrast, one year pre- and post-wild-land fire multi-temporal image showed the entire area encompassed in varied red color intensity, deep, and bright (Figure 3), indicating various possible levels of negative impact (Horning *et al.* 2010). Comparison of multi-temporal images illuminated significant visual differences between both time periods (Figure 3). While the seven year pre-wild-land fire multi-temporal image consisted of both positive and negative differences in growth potentials, the one year pre- and post-wild-land fire image revealed a uniquely comprised array of various shades and intensity of red, allowing for the latest technically advanced visually unique perspective of documented forest destruction (Figure 3) (Horning *et al.* 2010; Calfire 2010).

NDVI Imagery

One year pre-and post- NDVI images for Butte Humboldt and Lightning Complexes were incorporated into this study as another efficient and relatively quick tool to visually interpret fire impacts and landscape change (Horning *et al.* 2010). Comparison

of both Butte Humboldt and Lightning Complexes yielded significant differences in pre- and post-fire NDVI grey scale images. For example, the pre-fire NDVI image of Butte Lightning Complex affected areas revealed a semi-circular region of dark pixels indicative of decreased NDVI values and stressed vegetation and can be linked to the presence of prior recent fire disturbances (Figure 4) (Horning *et al.* 2010; van Leeuwen *et al.* 2010; Vicente-Serrano *et al.* 2011). In contrast, Butte Humboldt Complex affected areas, by the presence of light pixel regions, showed healthy vegetation with no visual signs of burn scars due to previous fire disturbances (Figure 2) (Horning *et al.* 2010). Comparison of both Complexes post-fire NDVI images gave a unique sense of scale and magnitude in relation to each other. A significantly larger and darker post-fire burn scar was observed for areas affected by the Butte Lightning Complex (Figure 4), which indicated greater vegetation damage and destruction (Horning *et al.* 2010) and may be attributed to the prior abundance of woody vegetation, typically observed in this mixed conifer forest area (Barbour and Major 1977). Vegetation types and post-fire vegetation re-growth dynamics are believed to have been contributing factors leading to less noticeable Butte Humboldt Complex burn scar and increased NDVI recovery (lighter pixels) (Figure 2) (Hernandez-Clemente *et al.* 2009; Horning *et al.* 2010; Vicente-Serrano *et al.* 2011). Results of the NDVI post-fire image comparisons between Complexes, however, may have been influenced by differences in NDVI recovery time because in efforts aimed at consistency, collection post-fire NDVI images for both Complexes were derived from a larger dated singular post-fire image, then transformed into NDVI grey-scale images (USGS 2010; Envi 4.8 2010). This inconsistency resulted in the Butte Humboldt Complex experiencing a longer recovery time due to image

acquisition date and prior containment in relation to the Butte Lightning Complex (Calfire 2010; USGS 2010).

Time Based NDVI and Climate Data Interpretation

The time based NDVI and climate data leading up to the Complexes of 2008 yielded interesting and informative results. During this twelve year pre-fire span, all subplots for both complexes observed NDVI temporal oscillations patterns indicative of the vegetation seasonality (Paruelo and Lauenroth 1995; Guerschman *et al.* 2003), which has been shown to be linked to climate fluctuations in precipitation and temperature (Gomez-Mendoza *et al.* 2008). Peak NDVI values were observed occurring at the height of vegetation growth around August, proceeded by minimum NDVI values occurring in the spring months of April and May (Figures 5 and 6). Timing of these NDVI temporal oscillation patterns corresponded with precipitation and maximum and minimum temperatures (Figures 5 and 6). More specifically, when precipitation was high, while minimum and maximum temperatures were low, decreased NDVI values were observed for the same time period, with an opposite trend observed for drier and hotter months (Figures 5 and 6). These results while adding further evidence to the relationship between NDVI and meteorological data, was not an unexpected outcome because of previously documented relationships between oscillation trends in NDVI values and meteorological variability (Gomez-Mendoza *et al.* 2008; van Leeuwen *et al.* 2010). There were however, several anomalies including decreases and increases of NDVI values as well as no data observed being inconsistent with associated seasonal oscillation patterns (Gomez-Mendoza *et al.* 2008). Closer examination revealed several trends that are consistent with

previous studies illustrating correlations between NDVI decreases and wild-land fire disturbance (van Leeuwen *et al.* 2010; Vicente-Serrano *et al.* 2011). For example, Butte Humboldt Complex unburned subplot two observed an increase in NDVI values on 6/5/2002, followed by a decrease to no data from 6/21/2002 to 08/24/2002 (Figure 5a). In addition, Butte Lighting Complex unburned one showed a significant decrease in NDVI values starting on 5/4/2002 and continuing through 8/24/2002 (Figure 6a). During this time period the presence of fire disturbance in Butte Humboldt Complex unburned two subplot area was verified through local fire records (Calfire 2010). Other decreased NDVI values were recorded for several subplots prior to the onset of Butte Humboldt and Lightning Complexes and may be contributed to one or many factors including fire disturbance, vegetation stress, decreased temperatures, increased precipitation, and cloud cover (Pettorelli *et al.* 2005; Zhong *et al.* 2010; Vicente-Serrano *et al.* 2011).

Prior studies have established relationships between lack of precipitation and drought to decreased NDVI values (Lloret *et al.* 2007; Gomez-Mendoza *et al.* 2008; van Leeuwen *et al.* 2010; Vicente-Serrano *et al.* 2011). Comparison of local meteorological data to NDVI values of burned center subplots leading up to of the onset of both Butte Humboldt and Lightning Complexes illustrated similar trends (Figures 5 and 6). Paradise weather stations noted low precipitation associated with drought-like conditions occurred for an extended time period prior to both wild-land fires (Figures 5 and 6) (NOAA 2010). BHC and BLC burned center subplots experienced normal NDVI values in the spring months of April and May prior to both fire disturbances (Figures 5 and 6) indicating gradual vegetation growth, due to relationships between NDVI and above ground net primary production (ANPP) (Paruelo and Lauenroth 1995). However, decreased NDVI

values were observed directly before both onsets for BHC and BLC, burn center subplots one and three and one and two respectively (Figures 5 and 6). A likely explanation could be related to a combination of drought-like conditions and elevated temperatures associated with mid-summer months, coupled with previous buildup of vegetation growth becoming drier and moisture stressed, led to decreased NDVI values prior to onset (Lloret *et al.* 2007; Gomez-Mendoza *et al.* 2008; van Leeuwen *et al.* 2010; Vicente-Serrano *et al.* 2011), which may have added significant influence on both ignition and nature of both fire disturbances (Pettorelli *et al.* 2005). Other fire studies have found similar results (Kobziar and Mcbride 2006). For example, the Lookout fire occurring in 1999, in north east areas of Plumas National Forest, caused extensive damage of over a thousand (ha) hectares with the onset attributed to lack of precipitation coupled with increased temperatures associated with early, mid, and late summer months (Kobziar and Mcbride 2006). During the temporal period when both Butte Complexes were active (Calfire 2010), NDVI values for BHC burned center subplots one and three and BLC burned center subplots one, two, and three decreased to no data (Figures 5 and 6). NDVI decreases of this nature indicate vegetation loss and exposure of bare rock and soil (Horning *et al.* 2010). Similar trends involving steep NDVI declines have been observed in *Pinus halepensis* forest affected areas (Vicente-Serrano *et al.* 2011).

NDVI post-fire recovery trends were clearly observed for both Butte Humboldt and Lightning Complex burned center subplots, though spatially different in nature. BHC burned center subplots showed a steady linear post-wild-land fire recovery with NDVI values peaking on 04/05/2009 (Figure 5c), while on the same date, BLC burned center two subplot had just started NDVI recovery with an initial recorded low

value after experiencing a no data period previously (Figure 6c). In addition, BLC burned center one and three subplots exhibited small gradual bell shaped curves, followed by all three BLC burned center subplots exhibiting steady increases in NDVI values (Figure 6c). Previous research has noted the possibility of full regeneration of forest type vegetation to pre-fire conditions in a time period of thirteen years following a major wild-land fire (Vicente-Serrano *et al.* 2011). Changes in species composition and initial increases in species abundance have been observed in the first stages of forest recovery (Kavgaci *et al.* 2010), on temporal scale of one to three years, followed by lower levels in subsequent years (Tarrega and Calabuig 1987; Hernandez-Clemente *et al.* 2009). However, increased levels of wild-land fire severity have been shown to decrease overall species abundance (Keeley *et al.* 2008). It is believed this initial post-fire temporal period which illustrated NDVI recovery for Butte Lightning Complex (Figure 6c), represents along with existing burned and partially burned vegetation, an understory re-growth consisting of herbs, forbs, and annuals, which have been shown to advantageously colonize previously unexposed areas (Kavgaci *et al.* 2010). Following this initial period, species abundance has been observed to decrease over time with increased competition from softwood and shrub species shaping the landscape (Kavgaci *et al.* 2010).

This 12-year retrospective analysis was able to illustrate post-wild-land fire NDVI recovery of vegetation to pre-wild-land fire NDVI levels. More specifically, BLC burned center three subplot exhibited a full recovery to pre-wild-land fire NDVI levels, with burned center one and two subplots exhibiting slightly less (Figure 5c). In contrast, even though the onset of BLC was documented approximately ten days later, BLC post-wild-land fire NDVI values for all three burned center subplots were not able to acheive

full recoveries during the course of this study (Figure 6c) (Calfire 2010). It is important to note, however, that while NDVI can temporally display overall vegetation responses in designated areas, limitations including lack of ability to individually discriminate plant types and sensitivities involved with mountainous terrain, slope, and aspect can affect spectrometer sensors and cause associated errors (Horning *et al.* 2010; Vicente-Serrano *et al.* 2011). Also, diverse elevations and plant community structure at subplot locations may have added further complications to NDVI results (Appendix A) (Gomez-Mendoza *et al.* 2008). Previous research has reported variability in NDVI results among different plant community types, related to different ranging elevations and weather conditions involving, cloud cover, temperature, and precipitation fluctuations occurring at individual locations (Gomez-Mendoza *et al.* 2008; Zhong *et al.* 2010). Additionally, van Leeuwen *et al.* 2010, pointed out the possibility that due to the short time span of twelve years pertaining to this time based study, trends associated with longer durations may not be distinguishable and or present.

Comparison of Satellite to Ground Based NDVI

Satellite to Ground based NDVI comparison by means of Coefficient of Determination (R^2) was accomplished for assessment of accuracy and validation of results (MS Excel 2010). Butte Humboldt Complex and Richardson Springs locations both showed weak positive linear correlations ($R^2 = 0.0859$) (Figure 7) and ($R^2 = 0$ .3555) (Figure 7) (MS Excel 2010). Results of previous ground validation approaches, comparing Landsat Satellite derived NDVI to field methods such the Composite Burn Index (CBI) index have yielded much stronger correlations ($R^2 = 0.79$) (Holden *et al.*

2010). Decisions for the non-utilization of Composite Burn Index (CBI) stemmed from limitations involving areas lacking forest vegetation and possible errors linked to its subjective quantitative nature (Veraverbeke *et al.* 2010), coupled with an opportunity to gain further understanding of portable spectrometer methods and applications. Nevertheless, future comparison of satellite NDVI and SRI data (excluded from this study) to CBI, may provide informative results (Veraverbeke *et al.* 2010).

Butte Lightning Complex showed a slightly negative linear correlation of (R^2 = .001) (Figure 7) (MS Excel 2010). Rocky and steep terrain as well as one hundred percent ground cover typical of this region may have contributed to field sampling errors at subplot locations (Barbour and Major 1977). Differences between satellite and ground based sampling elevations may also have influenced results in both wild-land fire affected areas (Gomez-Mendoza *et al.* 2008; Horning *et al.* 2010). For example, while satellite NDVI values were derived encompassing all vegetation in each individual pixel representing each 30 by 30 meter subplot, ground-based reflectance samples were collected approximately two meters from the ground, in an effort to maintain practicality and safety (Horning *et al.* 2010). This non-incorporation of abundance of burned and partially burned thin upper canopy and woody vegetation consistent with post-wild-land fire landscape typical of BLC (Barbour and Major 1977; Kavgaci *et al.* 2010), as well as sparsely dispersed oak canopies and upper shrub regions characteristic to BHC affected savannah-grassland and chaparral areas (Barbour *et al.* 1993), may likely have contributed to lack of robust correlations.

Interpretation of NBR and Delta Normalized Burn Ratio Results

The majority of pre- and post-NBR values for BHC and BLC unburned, burned edge subplots, were above zero indicating vegetation growth, resulting in delta NBR values corresponding to burn severities ranging from unburned to low re-growth (Table 1) (Miller and Thode 2007). This illustrated that these areas most likely either remained relatively unchanged or experienced slight increased vegetation growth (van Wagtendonk *et al.* 2004; Miller and Thode 2007). This is because negative pre- and post-NBR values would represent locations with no vegetation growth, more specifically would result in band 4 having a smaller reflectance in relation to band 7 (Miller and Thode 2007). BHC unburned three and BLC unburned two subplots observed delta NBR values indicating low-moderate burn severity (Table 1). BHC burned center three subplot observed delta NBR values indicating low re-growth, while in contrast, BLC burned center subplots two and three revealed high negative delta NBR values and thus could not be identified (Table 1) (Miller and Thode 2007). These results for BLC burned center subplots two and three were not expected because the delta NBR values were outside the known scale of -1 to 1 (Miller and Thode 2007). Although, technical inaccuracies involved with remote sensing procedures may not be ruled out (Kerr and Ostrovsky 2003), they may not be chiefly responsible due to consistency of all subplots using same remote sensing procedures and images (Appendix D) (Envi 2010; USGS 2010). Noted discrepancies, however, resided in high positive post-wild-land fire NBR values, particular to BLC burned center two and three subplots, thus effecting delta NBR values (Table. 1) (Miller and Thode 2007). However, through the use of a later post-NBR

acquisition date, NBR values for BLC burned center two and three subplots revealed normal ranges of post-NBR values (Miller and Thode 2007). Delta NBR values for BLC burned center two and three subplots in turn were consistent with low and mid to high burn severity levels respectively (Miller and Thode 2007).

Previous studies also have shown the NBR index can be sensitive to differences in types of vegetation classes (Epting *et al.* 2005). Relating to the Butte Lightning Complex affected areas, for example, results involving the Normalized Burn Ratio (NBR) have been shown to be more accurate for forest types in relation to savannah-grasslands areas, although post-fire forest areas with an abundance of burned woody material remnants may can cause spectral influences (Epting *et al.* 2005). An additional study found recovery in riparian areas in the mixed coniferous forest of Plumas National Forest to consist of focal competitors such as white fir sugar pine, Mountain Alder, Douglas fir, and red-osier dogwood (Kobziar and Mcbride 2006). These softwood vegetation types have been shown to prevail in post-fire re-growth and recovery and can be attributed to fire resistance capabilities, seed bank, and dispersal dynamics (Kobziar and Mcbride 2006). Post-wild-land fire vegetation re-growth in Savannah type grassland areas in contrast have been observed to be less predictable and inconsistent with broad areas of ranging from bare ground and sparse grasses and herbs to densely situated fire adapted shrubs and forbs which may have affected accuracy of results (Epting *et al.* 2005), and have led to discrepancies in results associated with similar approaches linking differenced NBR to fire severity (Keeley *et al.* 2008).

BHC burned center subplots one and two indicated low-severity burns, while in contrast, BLC burn center one subplot showed a zero post-NBR value, which in turn

resulted in a delta NBR value indicating low to moderate severity burn (Table 1) (Miller and Thode 2007). Previous research has established a wide range of possibilities for the lack of re-growth observed in BLC burned center one subplot and include quantities of sunlight, thickness and dimensions of pre-wild-land fire vegetation, angles of terrain, and elevation (Vicente-Serrano *et al.* 2011).

Previous fire severity assessments illustrated low severity levels for Sierra Nevada foothill and mountain regions, in relation to northern forest areas of Washington consisting of Western hemlock and Douglas-fir trees (Perry *et al.* 2011). The majority of burn severity levels for BHC and BLC, followed similar trends (Table 1) (Miller and Thode 2007); however, inaccuracies have been observed with delta NBR values in relation to post-wild-land fire landscapes (Smith *et al.* 2007). More specifically, vegetation indication by delta NBR values, when in turn, complete tree mortality occurred following fire disturbance (Smith *et al.* 2007). Also, in forest type areas known for moderate to high severity fires and complete stand destruction and increased variations in delta NBR values have been observed and attributed to swift post–wild-land fire recovery by vegetation understory re-growth (Smith *et al.* 2007). A previous study found a fire frequency ranging from five to ten years was ideal for forest health in areas consisting of white and red pines and over time may possibly reverse conditions in these areas which can be linked to present day wild-land fire outbreaks and severity (Neumann and Dickmann 2001). Additionally, fire impact studies in Plumas National Forest concluded that the amount of moisture content in the understory vegetation can play an important factor in fire severity level (Kobziar and Mcbride 2006; Kauffman and Martin 1989). Plant types also may influence fire severity levels (Kobziar and Mcbride 2006).

For example, Deer brush and Manzanita have been shown to burn with greater intensity than vegetation such as dogwood and alder (Kobziar and Mcbride 2006). Furthermore, forest ecosystems consisting of broader leaved trees have been shown to be less combustible in relation to denser areas of needle leaved trees (Epting *et al.* 2005).

Skinner and Chang's examinations of similar wild-land fire ecosystems may possibly allow for the broad characterizations of the post-wild-land fire BHC and BLC landscapes (Skinner and Chang 1996). For example, delta NBR indicating low severity for BHC burned center one and two subplots, may be generally described by low-land surface type fires, contrasted with elevated mortality of undersized trees (Skinner and Chang 1996). In contrast, delta NBR indications of low to moderate fire severity for BLC burned center one subplot may also be related and consistent with burned bark on surviving trees, along with significant destruction of undersized and crown tree species (Skinner and Chang 1996). Even though savannah and forest type areas affected by the Butte Humboldt and Lighting Complexes may be dissimilar in species and composition, they both however, occupy Mediterranean type ecosystems (Vicente-Serrano *et al.* 2011). Thus, they are comprised of numerous species of vegetation resistant and well fitted to fire disturbances, often utilizing specialized means involved with post-wild-land fire seedling re-emergence and denser less penetrable bark (Vicente-Serrano *et al.* 2011).

Using a two date approach to achieve delta NBR results instead of a single date indices post-wild-land fire method may also have contributed to host of errors influenced by differences in calibration of sensors between dates, atmospheric condition changes, and geometry involved between spectrometer sensors and the sun (Epting *et al.* 2005). Differences in vegetation types and changes in plant community dynamics also

may be attributed to possible errors associated with this method (van Wagtendonk *et al.* 2004). However, previous research illustrated that a two date approach may indeed be the preferred method for comparison, owing to increased accuracy in results (Epting *et al.* 2005).

CHAPTER VI

CONCLUSION

Recent increased frequencies of fire disturbances have prompted awareness and concerns leading to further demands for understanding of wild-land fire ecosystems and related dynamics (Whitlock *et al.* 2003). Assessments of Butte Humboldt and Lightning Complexes revealed insightful visual interpretations of landscape change through the use of innovative spectral techniques. These techniques included multi-temporal and NDVI grey-scale imagery, which have allowed for great potential and efficiency in evaluation and interpretation of landscape change over large areas (Horning *et al.* 2010). Noticeable levels of landscape change were observed for both BHC and BLC. BHC one year pre- and post-wild-land fire multi-temporal imagery displayed increased levels of negative impact in relation to imagery of seven year pre-wild-land fire. In contrast, BLC multi-temporal imagery of seven year pre-wild-land fire showed bright arrays of both negative and positive impact, while one year pre- and post-wild-land fire imagery revealed significant negative impact to encompassing vegetation. NDVI imagery also illustrated differences between BHC and BLC pre- and post-wild-land fire landscapes. BLC displayed a darker, more evident post-wild fire image burn scar in relation to BHC. In addition, only BLC showed evidence of a previous burn scar in pre-wild-land fire NDVI imagery, which may have influenced wild-land fire recovery and burn severity.

Previous research has shown similar time spans for NDVI and meteorological data comparison in wild-land fire affected areas to be small in comparison to long term prevalence of fire disturbances (van Leeuwen *et al.* 2010). This study's time-based NDVI and meteorological data comparison and analysis illustrated important pre- and post-wild-land fire trends. Timing of NDVI oscillations were observed to be related to temperature and precipitation fluctuations. Additionally, the onset of both wild-land fires may be linked to climate influences (van Leeuwen *et al.* 2010). More specifically, drought conditions prior to onset, giving rise to increased vegetation moisture stress, illustrated by NDVI decreases directly prior to ignition (Lloret *et al.* 2007; Gomez-Mendoza *et al.* 2008; van Leeuwen *et al.* 2010; Vicente-Serrano *et al.* 2011), directly impacting the likelihood of ignitions (Pettorelli *et al.* 2005). Post-wild-land fire NDVI values for both Complex subplots revealed vegetation recovery trends. BHC burned center three subplot was able to make a full recovery to pre-wild-land fire levels. BLC subplots showed initial post-wild-land fire NDVI recovery, suggestive of understory vegetation growth (Kavgaci *et al.* 2010), followed slow gradual increases. These differences in vegetation recovery rates may be attributed to increased post-wild-land fire re-growth typical of BHC savannah grassland affected areas (Hernandez-Clemente *et al.* 2009; Vicente-Serrano *et al.* 2011), along with extended recovery periods for larger softwood found in BLC forested areas (Barbour and Major 1977; Vicente-Serrano *et al.* 2011). Comparisons of satellite and ground based NDVI data using Coefficient of Determination R^2 correlations showed weak linear correlations for both Butte Humboldt Complex and Richardson Springs, while in contrast, slightly negative linear correlation observed for Butte Lighting Complex (MS Excel 2010). These poor correlations may be linked to differences in

optical sensor measurement heights (Gomez-Mendoza *et al.* 2008; Horning *et al.* 2010) and factors related to terrain accessibility (Barbour and Major 1977).

Normalized Burn Ratio (NBR) and delta Normalized Burn Ratio (dNBR) values yielded relevant insight into both BHC and BLC, fire affected ecosystems. According to the NBR and delta NBR scales outlined by Miller and Thode 2007, the majority of BHC and BLC pre- and post-wild-land fire NBR subplot values fell within acceptable positive values, indicating the presence of vegetation growth. Delta NBR values for most of the unburned and burned edge subplots resulted in burn severity levels ranging from low re-growth to unburned. Moreover, BHC burned center subplots results indicated burn severity levels of low and low re-growth. BLC burned center one subplot showed low to moderate burn severity levels, while BLC burned center subplots two and three could not be initially identified. However, a more recent post-NBR imagery of BLC burned center subplots two and three, revealed normal post-NBR values, with appropriate delta NBR values indicating low and mid to high burn severity levels.

This study's practical approach allowed for real world application and integration of biological principles with a variety of remote sensing techniques and applications. With the purpose of generating insightful and relevant results, which may be used to further understand landscape change and relationships between NDVI, climate, and ecosystem processes, in relation to wild-land fire disturbances. In addition, use of quantitative burn severity results added further perspective and enabled increased comprehension of dynamics related to wild-land fire affected areas (Miller and Thode 2007).

REFERENCES

REFERENCES

Barbour MG, Major J (1977) 'Terrestrial vegetation of California'. pp. 18-906. (University of California Davis: Davis, CA)

Barbour MG, Pavlik B, Drysdale F, Lindstrom S (1993) 'California's changing landscapes: diversity and conservation of California vegetation'. pp. 1-185. (California Native Plant Society: Sacramento, CA)

Black SC, Guo X (2008) Estimation of grassland CO_2 exchange rates using hyperspectral remote sensing techniques. *International Journal of Remote Sensing* **29**, 145-155. doi:10.1080/01431160701253220

Calfire (2010) Internet source: www.fire.cal.gov/ Accessed on March 15, 2010.

Conedera M, Tinner W, Neff C, Meurer M, Dickens A, Krebs P (2008) Reconstructing past fire regimes: methods, applications, and relevance to fire management and conservation. *Quaternary Science Reviews* **28**, 555-576. doi:10.1016/j.quascirev.2008.11.005

Dobrowski SZ, Pushnik JC, Zarco-Tejada PJ, Ustin SL (2005) Simple reflectance indices track heat and water stress-induced changes in steady-state chlorophyll fluorescence at the canopy scale. *Remote Sensing of Environment* **97**, 403-414. doi:10.1016/j.rse.2005.05.006

Envi 4.8 (2010) Exelis visual information solutions. Boulder, CO. Web address: www.exelisvis.com

Epting J, Verbyla D, Sorbel B (2005) Evaluation of remotely sensed indices for assessing burn severity in interior Alaska using Landsat TM and ETM+. *Remote Sensing of Environment* **96**, 328-339. doi:10.1016/j.rse.2005.03.002

Erlandson JM (1994) 'Interdisciplinary Contributions to Archaeology: Early hunter gatherers of the California coast'. pp. 1-311. (Plenum Press: New York)

Filella I, Penuelas J, Llorens L, Estiarte M (2004) Reflectance assessment of seasonal and annual changes in biomass and $C0_2$ uptake of Mediterranean shrubland submitted to experimental warming and drought. *Remotes Sensing of Environment* **90**, 308-318. doi:10.1016/j.rse.2004.01.010

Fried J, Torn M, Mills E (2004) The impact of climate change on wildfire severity: a regional forecast for Northern California. *Climate Change* **64**, 161-191. doi:10.1023/B:CLIM.0000024667.89579.ed

Fry D, Stephens S (2006) Influences of humans and climate on the fire history of a ponderosa pine mixed conifer forest in the southeastern Klamath Mountains, California. *Forrest Ecology and Management* **223**, 428-438. doi:10.1016/j.foreco.2005.12.021

Garmin (2008) Garmin International Inc. Olathe, KS 66062. Web address: www.gramin.com/

Gomez-Mendoza L, Galicia L, Cuevas-Fernandez ML, Magana V, Gomez G, Palacio-Prieto JL (2008) Assessing onset and length of greening period in six vegetation types in Oaxaca, Mexico, using NDVI-precipitation relationships. *International Journal Biometeorol* **52**, 511-520. doi:10.1007/s00484-008-0147-6

Guerschman JP, Paruelo JM, Burke IC (2003) Land use impacts on the normalized vegetation index in temperate Argentina. *Ecological applications* **13**, 616-628. doi:10.1890/1051-0761(2003)013[0616:LUIOTN]2.0.CO;2

Hernandez-Clemente R, Navarro Cerrillo RM, Hernandez-Bermejo JE, Escuin Royo S, Kasimis NA (2009) Analysis of postfire vegetation dynamics of Mediterranean shrub species based on terrestrial and NDVI data. *Environmental Management* **43**, 876-887. doi:10.1007/s00267-008-9260-x

Holden ZA, Morgan P, Smith AM, Vierling L (2010) Beyond Landsat: a comparison of four satellite sensors for detecting burn severity in ponderosa pine forests of the Gila Wilderness, NM, USA. *International Journal of Wildland Fire* **19**, 449-458. doi:10.1071/WF071061049-8001/10/040449

Horning N, Robinson JA, Sterling EJ, Turner W, Spector S (2010) 'Remote sensing for ecology and conservation: a handbook of techniques'. pp. 4-371. (Oxford University Press: New York)

Inoue Y (2003) Synergy of remote sensing and modeling for estimating ecophysiological processes in plant production. *Plant Production Science* **6**, 3-16. doi:10.162/pps.6.3

Jenkins M (2011) Physiological effects of sulphur dioxide induced stress on vegetation under natural conditions. Master Thesis, California State University Chico. (Chico, CA) http://hdl.handle.net/10211.4/314

Jones TL, Kennett DJ (1999) Late Holocene sea temperatures along the central California coast. *Quaternary Research* **51**, 74-82. doi:10.1006/qres.1998.2000

Kavgaci A, Carni A, Basaran S, Basaran MA, Kosir P, Marinsek A, Silc U (2010) Long-term post- fire succession of *Pinus brutia* forest in the east Mediterranean. *International Journal of Wildland Fire* **19**, 599-605. doi:10.1071/WF080441049-8001/10/050599

Keeley J (2000) Chaparral. In 'North American Terrestrial Vegetation'. (Eds MG Barbour, WD Billings) pp. 203-254. (Cambridge University Press: United Kingdom)

Keeley J (2002) Native American impacts on fire regimes of the California coastal ranges. *Journal of Biogeography* **29**, 303-320. doi:10.1046/j.1365-2699.2002.00676.x

Keeley JE, Brennan T, Pfaff AH (2008) Fire severity and ecosystem responses following crown fires in California shrublands. *Ecological Applications* **18**, 1530-1546. doi:10.1046/j.1365-2699.2002.00676.x

Keeley JE, Fotheringham CJ (1998) Smoke induced seed germination in California chaparral. *Ecology* **79**, 2320-2336. doi:10.1890/0012-9658(1998)079[2320:SISGIC12.0.CO;2

Kennedy R, Wimberly M (2009) Historical fire and vegetation dynamics in dry forests of the interior Pacific Northwest, USA, and relationships to Northern Spotted Owl (*Strix occidentalis*) habitat conservation. *Forest Ecology and Management* **258**, 554-566. doi:10.1016/j.foreco.2009.04.019

Kerr JT, Ostrovsky M (2003) From space to species: ecological applications for remote sensing. *Trends in Ecology and Evolution* **18**, 299-305. doi:10.1016/S0169-5347(03)00071-5

Key CH, Benson NC (2006) 'Landscape assessment: sampling and analysis methods: Firemon: fire effects monitoring and inventory system. General Technical Report'. USDA Forest Service, Rocky Mountain Research Station, Fort Collins CO, RMRS-GTR-164-CD.

Kneeshaw K, Vaske J, Bright A, Absher J (2004) Acceptability norms toward fire management in three national forest. *Environment and Behavior* **36**, 592-612. doi:10.1177/0013916503259510

Kobziar LN, McBride JR (2006) Wildfire burn patterns and riparian vegetation response along two northern Sierra Nevada streams. *Forest Ecology and Management* **222**, 254-265. doi:10.1016/j.foreco.2005.10.024

Letts MG, Phelan CA, Johnson DRE, Rood SB (2008) Seasonal photosynthetic gas exchange and leaf reflectance characteristics of male and female cottonwoods in a riparian woodland. *Tree Physiology* **28**, 1037-1048. doi:10.1093/treephys/28.7.1037

Lichtenhaler HK, Wenzel O, Buschmann C, Gitelson A (1998) Plant stress detection by reflectance and fluorescence. *Annals of the New York Academy of Sciences* **851**, 271-285. doi:10.1111/j.1749-6632.1998.tb09002.x

Lloret F, Lobo A, Estevan H, Maisongrande P, Vayreda J, Terradas J (2007) Woody plant richness and NDVI response to drought events in Catalonian (northeastern Spain) forests. *Ecology* **88**, 2270-2279. doi:10.1890/06-1195.1

Microsoft Excel (2010) Microsoft Corporation. One Microsoft Way, Redmond, Washington 98052. Web address: www.microsoft.com/

Miller JD, Thode AE (2007) Quantifying burn severity in a heterogeneous landscape with a relative version of the data Normalized Burn Ratio (dNBR). *Remote Sensing of Environment* **109**, 66-80. doi:10.1016/j.rse.2006.12.006

Neumann DD, Dickmann DI (2001) Surface burning in a mature stand of *Pinus resinosa* and *Pinus strobus* in Michigan: effects on understory vegetation. *International Journal of Wildland Fire* **10**, 91-101. doi:10.1071/WF010211049-8001/01/010091

NOAA – National Oceanic and Atmospheric Administration (2010) Internet source: www.noaa.gov/ Accessed on February 15, 2010.

Paruelo JM, Lauenroth WK (1995) Regional patterns of Normalized Difference Vegetation Index in North American shrublands and grasslands. *Ecology* **76**, 1888-1898.

Perry DA, Hessburg PF, Skinner CN, Spies TA, Stephens SL, Taylor AH, Franklin JF, McComb B, Riegel G (2011) The ecology of mixed severity fire regimes in Washington, Oregon, and Northern California. *Forest Ecology and Management* **262**, 703-717. doi:10.1016/j.foreco.2011.05.004

Pettorelli N, Olav Vik J, Mysterud A, Gaillard JM, Tucker CJ, Stenseth NC (2005) Using the satellite-derived NDVI to assess ecological responses to environmental change. *Trends in Ecology and Evolution* **20**, 503-510. doi:10.1016/j.tree.2005.05.011

Ritchie M, Skinner C, Hamilton T (2007) Probability of tree survival after wildfire in an interior pine forest of northern California: effects of thinning and prescribed fire. *Forest Ecology and Management* **247**, 200-208. doi:10.1016/j.foreco.2007.04.044

Rosso PH, Pushnik JC, Lay M, Ustin SL (2005) Reflectance properties and physiological responses of *Salicornia virginica* to heavy metal and petroleum contamination. *Environmental Pollution* **137**, 241-252. doi:10.1016/j.envpol.2005.02.025

Roughgarden J, Running SW, Matson PA (1991) What does remote sensing do for ecology. *Ecology* **72**, 1918-1922.

Salazar L, Kogan F, Roytman L (2007) Use of remote sensing data for estimation of winter wheat yield in the United States. *International Journal of Remotes Sensing* **28,** 3795-3811. doi:10.1080/01431160601050395

Santos MJ, Greenberg JA, Ustin SL (2010) Using hyperspectral remote sensing to detect and quantify southeastern pine senescence effects in red-cockaded woodpecker (*Picoides borealis*) habitat. *Remote Sensing of Environment* **114**, 1242-1250. doi:10.1016/j.rse.2010.01.009

Sims DA, Gamon JA (2003) Estimation of vegetation water content and photosynthetic tissue area from spectral reflectance: a comparison of indices based on liquid water and chlorophyll absorption features. *Remote Sensing of Environment* **84**, 526-537. doi:10.1016/S0034-4257(02)00151-7

Skinner C, Chang C (1996) Fire regimes, past and present. Sierra Nevada Ecosystem Project: final report to Congress. Internet Source: http://gis.fs.fed.us/psw/programs/ecology_of_western_forest/publications/publications/1996-01-SkinnerChang.pdf Accessed on October 1, 2009.

Smith AMS, Lentile LB, Hudak AT, Morgan P (2007) Evaluation of linear spectral unmixing and ΔNBR for predicting post-fire recovery in a North American ponderosa pine forest. *International Journal of Remote Sensing* **28**, 5159-5166. doi:10.1080/01431160701395161

Soverel NO, Perrakis DDB, Coops NC (2010) Estimating burn severity for Landsat dNBR and RdNBR indices across western Canada. *Remote Sensing of Environment* **114**, 1896-1909. doi:10.1016/j.rse.2010.03.013

Tarrega R, Calabuig EL (1987) Effects of fire on structure dynamics and regeneration of *Quercus pyrenaica* ecosystems. *Ecologia Mediterranea* **13**, 79-86.

Taylor A, Beaty R (2005) Climate influences of fire regimes in northern Sierra Nevada mountains, Lake Tahoe Basin, Nevada, USA. *Journal of Biogeography* **32**, 425-438. doi:10.1111/j.1365-2699.2004.01208.x

Taylor A, Skinner C (1998) Fire history and landscape dynamics in a late successional reserve, Klamath Mountains, California, USA. *Forest Ecology and Management* **111**, 285-301. doi:10.1016/S0378-1127(98)00342-9

Tucker CJ (1979) Red and photographic infrared linear combinations for monitoring vegetation. *Remote sensing of Environment* **8**, 127-150. doi:10.1016/0034-4257(79)90013-0

Unispec SC (2008) PP Systems International Inc. Amesbury, MA. Web address: www.ppsystems.com

USGS – U.S. Geological Survey (2011) Internet source: www.usgs.gov/ Accessed on February 15, 2010.

Ustin SL, Gamon JA (2010) Remote sensing of plant functional types. *New Phytologist* **186**, 795-816. doi: 10.1111/j.1469-8137.2010.03284.x

van Leeuwen WJD, Casady GM, Neary DG, Bautista S, Alloza JA, Carmel Y, Wittenberg L, Malkinson D, Orr BJ (2010) Monitoring post-wildfire vegetation response with remotely sensed time series data in Spain, USA and Israel. *International Journal of Wildland Fire* **19**, 75-93. doi: 10.1071/WF080781049-8001/10/010075

van Wagtendonk JW, Root RR, Key CC (2004) Comparison of AVIRIS and Landsat ETM+ detection capabilities for burn severity. *Remote Sensing of Environment* **92**, 397-408. doi:10.1016/j.rse.200312.015

Veraverbeke S, Verstraeten WW, Lhermitte S, Goossens R (2010) Evaluating Landsat Thematic Mapper spectral indices for estimating burn severity of the 2007 Peloponnese wildfires in Greece. *International Journal of Wildland Fire* **19**, 558-569. doi:10.1071/WF090691049-8001/10/050558

Vicente-Serrano SM, Perez-Cabello F, Lasanta T (2011) *Pinus halepensis* regeneration after a wildfire in a semiarid environment: assessment using multitemporal Landsat images. *International Journal of Wildland Fire* **20**, 195-208. doi:10.1071/WF082031049-8001/11/020195

Whitlock C, Shafer SL, Marlon J (2003) The role of climate and vegetation change in shaping past and future fire regimes in the northwestern US and the implications for ecosystem management. *Forest Ecology and Management* **178**, 5-21. doi:10.1016/S0378-1127(03)00051-3

Yilmaz MT, Hunt ER Jr., Goins LD, Ustin SL, Vanderbilt VC, Jackson TJ (2008) Vegetation water content during SMEXo4 from ground data and Landsat 5 Thematic Mapper imagery. *Remote Sensing of Environment* **112**, 350-362. doi: 10.1016g.rse2007.03.020

Zhong L, Ma Y, Suhyb Salama M, Su Z (2010) Assessment of vegetation dynamics and their response to variations in precipitation and temperature in the Tibetan Plateau. *Climate Change* **103**, 519-535. doi: 10.1007/s10584-009-9787-8

Zomer RJ, Trabucco A, Ustin SL (2009) Building spectral libraries for wetlands land cover classification and hyperspectral remote sensing. *Journal of Environmental Management* **90**, 2170-2177. doi: 10.1016/j.jenvman.2007.06.028

APPENDIX A

SUBPLOT COORDINATES

AND ELEVATIONS

Butte Humboldt Complex	Latitude	Longitude	Elevation (ft)
reference	39°42.7080	-121°46.7739	242
unburned 1	39°44.7436	-121°39.6569	1387
unburned 2	39°40.6800	-121°43.7200	416
unburned 3	39°43.7280	-121°39.6560	1207
burned edge 1	39°44.7355	-121°46.7703	309
burned edge 2	39°42.7051	-121°44.7360	511
burned edge 3	39°41.6900	-121°42.7020	587
burn center 1	39°43.7240	-121°41.6920	1023
burn center 2	39°43.7310	-121°40.6808	1125
burn center 3	39°42.7080	-121°40.6770	908

Butte Lightning Complex	Latitude	Longitude	Elevation (ft)
reference	39°40.1750	-121°31.5630	1049
unburned 1	39°43.7260	-121°30.5080	1876
unburned 2	39°42.7163	-121°31.5216	1991
unburned 3	39°42.7045	-121°31.5295	1853
burned edge 1	39°45.7610	-121°28.4770	2080
burned edge 2	39°47.7970	-121°26.4490	1522
burned edge 3	39°53.8880	-121°21.3630	1666
burn center 1	39°47.7983	-121°29.4875	2755
burn center 2	39°47.7986	-121°29.4911	2667
burn center 3	39°47.7973	-121°29.4934	2543

Richardson Springs	Latitude	Longitude	Elevation (ft)
1c	39°50.8330	-121°48.8050	413
2c	39°50.8350	-121°48.8020	433
3c	39°50.8370	-121°47.7990	498
4c	39°50.8390	-121°47.7960	518
5c	39°50.8390	-121°47.7930	547
6c	39°50.4590	-121°47.2770	587
7c	39°50.4620	-121°47.1260	600
8c	39°49.6390	-121°49.7110	357
9c	39°49.5890	-121°49.9730	356
10c	39°49.1870	-121°50.6320	301

APPENDIX B

UNISPEC SC (PORTABLE REMOTE SENSING SPECTROMETER) INSTRUCTIONS

1. Before Unispec SC is turned on, attach two fiber optic cables to the rear portion of the device.
2. Press the on switch, and starting program should become visible. If starting program does not become visible, then touch “refresh button” on the right upper side of the screen.
3. Allow the Unispec SC ten to fifteen minutes to warm up and get used the surroundings.
4. In order for communication to take place between the fiber optic cables and the machine, under “scans” heading, press “data scan” or number 2.
5. In the “setup” heading, proceed to “Measurement preferences” and set parameters for “Halogen source intensity” at 0%, “average scans” at 40, and “integration time” at 100.
6. In order to save data two options are available. Proceed to “file” heading and under “Save data” decide which directory to save data. Or proceed to “setup” heading and go to “Measurement preferences.” Then adjust “Default directory and data file” appropriately to decide where data will be saved.
7. Under the heading “scans,” go to “dark scan” and select after applying optic cover.
8. Before future scans, use and record white board data by going to “scans” and selecting “reference scan.” Press “data scans” to record field data.
9. In order to view and transfer field data, go to “file,” select “flashFX Disk” and then under “usScfvl_2,” select “data file” and then “all documents,” select desired document. Data then can be uploaded to computer for calculating reflectance and NDVI values.

* (Modified from Jenkins 2011, Master Thesis)

APPENDIX C

REMOTE SENSING PROCEDURE FOR

OBTAINING NDVI VALUES

1. Under Envi 4.8 software press enter to start program.
2. Go to “external file,” under “Landsat” select “geotiff.”
3. Proceed to “documents” (Where images are stored on hard drive) select desired individual image (images one through eighty-five).
4. Under individual image, highlight all seven sub images and press “open.”
5. Proceed to the header “basic tools” and select “layer stacking.”
6. Under “layer stacking” select “import file,” then highlight all files and select “ok.”
7. Go to “output file name,” create image file name and select “ok.”
8. A box will appear showing the image file name, highlight “image name.”
9. Under “edit header,” proceed to “edit attributes” and select “wavelengths.”
10. Select “edit wavelength values” and assign specific wavelength numerical values to each of the bands one through seven, then select “Ok.”
11. Proceed to the header “transform” and under “NDVI” select image.
12. Choose “output file,” then create file name with a suffix of “.dat,” then select “ok.”
13. Proceed to the header “spectral vegetation analysis” and select “vegetation index calculator.”
14. Select “impute file,” then highlight all available bands.
15. Proceed to “vegetation index parameters,” select “NDVI” or “SRI.”
16. Go to “output file,” select “ok.”
17. Select individual file of interest with “.dat” suffix and image will be displayed.
18. Select “pixel locator” box and enter in latitude and longitude of individual subplot location, then choose “apply.”
19. Center the cursor in subplot and record numerical value.
20. For every individual image, steps 1-19 need to be repeated.

APPENDIX D

PROCEDURE TO OBTAIN NORMALIZED BURN RATIO VALUES

1. Repeat steps one through ten in Appendix E.
2. Open image and precede to the header “basic tools,” then select” band math.”
3. Under “band math” enter in mathematical expression “float (b4-b7)/ (b4+b7).”
4. Go to “map variable impute file,” then select “b4 single band” and “b7 single band.”
5. Enter “output file name” with “.dat” as the suffix.
6. Highlight “band math” and select “grey-scale load.”
7. Proceed to “tools” and select “pixel locator” box and enter in latitude and longitude of individual sub-plot locations.
8. Center cursor in subplot location and record numerical value.

APPENDIX E

PICTURES OF VARIOUS BHC AND

BLC SUBPLOT LOCATIONS

1. Butte Lightning Complex burned center

2. Butte Humboldt Complex burned edge

3. Richardson Springs

4. Butte Lightning Complex burned center